EUROPEAN RESPIRATORY journal

FLAGSHIP SCIENTIFIC JOURNAL OF ERS

Early View

Original research article

Nestin promotes pulmonary fibrosis *via* facilitating recycling of TGF-β receptor I

Jiancheng Wang, Xiaofan Lai, Senyu Yao, Hainan Chen, Jianye Cai, Yulong Luo, Yi Wang, Yuan Qiu, Yinong Huang, Xiaoyue Wei, Boyan Wang, Qiying Lu, Yuanjun Guan, Tao Wang, Shiyue Li, Andy Peng Xiang

Please cite this article as: Wang J, Lai X, Yao S, *et al*. Nestin promotes pulmonary fibrosis *via* facilitating recycling of TGF-β receptor I. *Eur Respir J* 2021; in press (https://doi.org/10.1183/13993003.03721-2020).

Nestin promotes pulmonary fibrosis *via* facilitating recycling of TGF-β receptor I

Jiancheng Wang[1,2,3,11], Xiaofan Lai[2,4,11], Senyu Yao[2,11], Hainan Chen[2,11], Jianye Cai[2,5], Yulong Luo[6], Yi Wang[2], Yuan Qiu[2], Yinong Huang[2,7], Xiaoyue Wei[2], Boyan Wang[2], Qiying Lu[2], Yuanjun Guan[8], Tao Wang[2], Shiyue Li[6,*], Andy Peng Xiang[2,9,10,*].

[1] Scientific Research Center, The Seventh Affiliated Hospital of Sun Yat-sen University, Shenzhen, China.

[2] Center for Stem Cell Biology and Tissue Engineering, Key Laboratory for Stem Cells and Tissue Engineering, Ministry of Education, Sun Yat-Sen University, Guangzhou, China.

[3] Department of Hematology, The Seventh Affiliated Hospital, Sun Yat-Sen University, Shenzhen, China.

[4] Department of Anesthesiology, The First Affiliated Hospital, Sun Yat-sen University, Guangzhou, China.

[5] Department of Hepatic Surgery and Liver Transplantation Center of the Third Affiliated Hospital, Organ Transplantation Institute, Sun Yat-Sen University, Guangzhou, China.

[6] National Clinical Research Center for Respiratory Disease, State Key Laboratory of Respiratory Disease, Guangzhou Institute of Respiratory Health, the First Affiliated Hospital of Guangzhou Medical University, Guangzhou, China.

[7] Department of Endocrinology, The First Affiliated Hospital of Sun Yat-Sen University, Guangzhou, China.

[8] Core Facility of Center, Zhongshan School of Medicine, Sun Yat-Sen University, Guangzhou, China.

[9] Department of Biochemistry, Zhongshan School of Medicine, Sun Yat-Sen University, Guangzhou, China.

[10] Center for Precision Medicine, Sun Yat-Sen University, Guangzhou, China.

[11] These authors contributed equally to this work.

***Corresponding author:**

Dr Andy Peng Xiang, Phone: 86-20-87335822, E-mail: xiangp@mail.sysu.edu.cn

Dr Shiyue Li, Phone: 86-20-83062885, E-mail: lishiyue@188.com

Summary:

Nestin regulates the vesicular trafficking system by promoting Rab11-dependent recycling of TβRI and thereby contributes to the progression of pulmonary fibrosis. Precise targeting of Nestin may represent a potential therapeutic strategy for IPF.

Abstract

Idiopathic pulmonary fibrosis (IPF) is a progressive fibrotic lung disease that is characterized by aberrant proliferation of activated myofibroblasts and pathological remodelling of the extracellular matrix. Previous studies have revealed that the intermediate filament protein Nestin plays key roles in tissue regeneration and wound healing in different organs. Whether Nestin plays a critical role in the pathogenesis of IPF needs to be clarified.

Nestin expression in lung tissues from bleomycin-treated mice and IPF patients was determined. Transfection with Nestin shRNA vectors in vitro that regulated TGF-β/Smad signalling was conducted. Biotinylation assays to observe plasma membrane TβRI, TβRI endocytosis and TβRI recycling after Nestin knockdown were performed. Adeno-associated virus serotype 6 (AAV6)-mediated Nestin knockdown was assessed in vivo.

We found that Nestin expression was increased in a murine pulmonary fibrosis model and IPF patients, and that the upregulated protein primarily localized in lung α-SMA^{+} myofibroblasts. Mechanistically, we determined that Nestin knockdown inhibited TGF-β signalling by suppressing recycling of TβRI to the cell surface and that Rab11 was required for the ability of Nestin to promote TβRI recycling. In vivo, we found that intratracheal administration of adeno-associated virus serotype 6 (AAV6)-mediated Nestin knockdown significantly alleviated pulmonary fibrosis in multiple experimental mice models.

In conclusion, our findings reveal a pro-fibrotic function of Nestin partially through facilitating Rab11-dependent recycling of TβRI and shed new light on pulmonary fibrosis treatment.

Introduction

Pulmonary fibrosis is a pathological outcome of many chronic inflammatory and autoimmune pulmonary diseases. The most common form of pulmonary fibrosis, idiopathic pulmonary fibrosis (IPF), is characterized by alveolar epithelial cell injury, fibroblast proliferation, myofibroblast differentiation, and progressive collagen deposition, eventually leading to organ malfunction and death [1-4]. Currently, there is still a lack of an effective medical therapy for IPF, in part because its pathogenic mechanisms remain unclear [5]. Thus, it is urgent to explore the exact molecular mechanism underlying IPF progression, with the goal of developing new treatments.

Nestin is a type VI intermediate filament protein that was originally identified in neural progenitor/stem cells of the developing central nervous system [6, 7]. Recent studies have shown that Nestin is not only a common marker of multi-lineage stem cells, but also plays direct biological roles in active proliferation and tissue regeneration in different tissues and organs [8, 9]. Our previous studies showed that Nestin could regulate the structural and functional homeostasis of mitochondria [10]. We also demonstrated that Nestin regulated the antioxidant capacity of cells through the Keap1-Nrf2 feedback loop [11] and that nuclear Nestin regulated the homeostasis of nuclear lamin A/C and contributed to cellular senescence [12]. In addition, Nestin was also reported to participate in the pathogenesis of fibrosis in multiple organs. For example, Nestin expression was increased in activated rat hepatic stellate cells, fibrotic kidney and heart tissues [13-15], suggesting that it might be an activation marker of tissue fibrosis. However, the exact molecular mechanisms through which Nestin contributes to pulmonary fibrosis remain poorly understood.

Transforming growth factor-β (TGF-β) is a multifunctional cytokine that has been shown to play crucial roles in the pathogenesis of organ fibrosis [16, 17]. TGF-β activates the phosphorylation of Smad by TGF-β receptor I (TβRI) and TGF-β receptor II (TβRII) [16]. Furthermore, phosphorylated Smad translocates into the nucleus, where it modulates the transcription of downstream target genes, including alpha-smooth muscle actin (α-SMA) and Collagen I [17]. Abundant evidence has demonstrated that endocytosis and trafficking of TGF-β receptors significantly regulate the activation of TGF-β intracellular signalling [18-20]. Endosomal TGF-β receptors follow two trafficking routes in cells: some are recycled to the plasma membrane, while others are sorted to late endosomes/lysosomes for degradation [21]. In addition, small Ras-like GTPases are well-recognized regulators of various membrane trafficking events [22-24]. For instance, Rab11 and Rab4 are known to play essential roles in regulating recycling endosomes [25]. Therefore, whether Nestin participates in the endocytosis and trafficking of TGF-β receptors still needs to be clarified.

Here, we detected the expression and localization of Nestin in the lungs of bleomycin-induced murine pulmonary fibrosis model mice and IPF patients, and investigated the potential role of Nestin in regulating TGF-β/Smad signalling and Rab11-mediated TβRI recycling. We also addressed whether targeting Nestin could be an attractive strategy for attenuating pulmonary fibrosis in vivo.

Material and methods

A detailed description of methods is provided in the online data supplement.

Animal experiments

Animal use was approved by the Ethical Committee of Sun Yat-sen University. C57BL/6 mice were purchased from Beijing Vital River Laboratory. Nestin-GFP mice (expressing Nestin promoter-driven GFP in the C57BL/6 genetic background) were provided by Dr. Masahiro Yamaguchi [26]. All mice were provided free access to food and water and kept in a colony room on a 12:12 hour light/dark cycle in the Sun Yat-sen University Animal Center. For bleomycin or amiodarone instillation, 8-week-old mice were anesthetized with isoflurane and intratracheally injected with bleomycin (Teva Pharmaceutical; 3 U/kg) or with amiodarone (Sigma-Aldrich; 0.8mg/kg/5d). Control groups received injections with an equal volume of PBS or 4% Ethanol. TGF-β1–overexpression lung fibrosis model was described previously [27, 28]. Adenovirus expressing constitutively active TGF-β1 and control virus vector were purchased from the Hanbio Biotechnology Co., Ltd (Shanghai, China). For AdTGF-β1 instillation, 8-week-old mice were anesthetized with isoflurane and intratracheally injected with AdTGF-β1 (1.5×10^{12} pfu) or with Advector (1.5×10^{12} pfu).

Study population

Human lung tissues with fibrosis were obtained by diagnostic surgical lung biopsies from patients who fulfilled the diagnostic criteria for IPF at the First Affiliated Hospital of Guangzhou Medical University, Guangzhou, China. Control human lung tissue samples were collected from surgical lung resection from patients with lung cancer at the same hospital. All patients signed informed consent for their samples to be used

for research, and approval was obtained from the Committees for Ethical Review of Research.

Statistics

All data are reported as the mean ± SD of at least three independent experiments. Sample sizes are all presented in the figure legends. Statistical analysis between two groups was performed using unpaired *t*-test. Statistical analysis between multiple groups was performed by one-way ANOVA, with Tukey's multiple comparison test. All data were analyzed using Prism software (GraphPad Software). Statistical significance was taken as a P value less than 0.05, with significance defined as $P < 0.05$ (*) $P < 0.01$ (**) $P < 0.001$ (***).

Results

Nestin is upregulated in experimental pulmonary fibrosis and localizes mainly in lung myofibroblasts

First, we confirmed that bleomycin instillation led to lung collagen deposition and fibrosis, as demonstrated by H&E, Masson trichrome and α-SMA staining. Meanwhile, we found that Nestin protein levels and the proportion of $Nestin^+$ cells gradually increased during the development of lung fibrosis (figure 1a-c and supplementary figure S1a-b). Then, we further confirmed that both mRNA and protein levels of Nestin increased markedly in fibrotic lung tissues as the degree of lung fibrosis increased (figure 1d-f). In addition, analysis of bulk RNA-sequence data from GSE110533 revealed significant upregulation of Nestin in bleomycin-induced lung fibrosis mice [29] (supplementary figure S1c). Also, overexpression of Nestin observed in bleomycin-induced pulmonary fibrosis was predominantly localized to lung

myofibroblasts, as validated by flow cytometry and immunofluorescent staining (supplementary figure S1d and figure 1g-j). Besides, the above findings were further evidenced by single-cell RNA-seq analyses from GSE132771 [30] (supplementary figure S1e-i). We also found that some Nestin+ cells co-expressed pericyte marker (NG2+) or smooth muscle cell marker (Calponin 1+) in lung tissues and there was a slight increase of these two cell types in pulmonary fibrosis, although the percentage of Nestin+NG2+ and Nestin+Calponin 1+ cells in all Nestin+cells decreased (figure 1g-j). Meanwhile, there was little-to-no colocalization between Nestin and CD31 (vascular endothelial cells), SPC (type II alveolar epithelial cells) or AQP5 (type I alveolar epithelial cells) (figure 1g-j). These results suggested that Nestin expression in lung myofibroblasts is positively correlated with the severity of pulmonary fibrosis.

Nestin is upregulated in the lungs of patients with IPF

Next, we examined Nestin expression in the lungs of IPF patients and healthy donors. Similarly, we found that Nestin was markedly overexpressed in IPF fibrotic lungs compared with normal lungs (figure 2a-e). This was further confirmed by bulk RNA-sequence data analysis of lungs from IPF samples and control samples from GSE124685 [31] (supplementary figure S2a). Single-cell RNA-seq data from GSE132771 also proved the similar phenomenon as in mice [30] (supplementary figure S2b-f). Also, we analysed the correlation between Nestin expression in patients with IPF and certain clinical lung function test parameters. Interestingly, Nestin expression was negatively correlated with TLC% pred, DLCO% pred, FEV1% pred and FVC% pred (figure 2f-i, supplementary table S1 and S2). Furthermore, immunofluorescence (IF) assays and single-cell RNA-seq analysis both revealed that Nestin was primarily expressed in myofibroblasts, as evidenced by colocalization with

both α-SMA and Collagen I (figure 2j-m and supplementary figure S2b-h). The results suggested that Nestin may play an important role in regulating the progression of idiopathic pulmonary fibrosis.

Nestin knockdown inhibits the TGF-β/Smad signaling pathway

Next, we isolated primary fibroblasts from the lungs of mice and evaluated the functions of Nestin. First, Nestin was significantly downregulated in primary mouse lung fibroblasts subjected to Nestin knockdown by two different short hairpin RNAs (shRNAs) and the TGFβ-inducible SBEs luciferase activities were accordingly decreased (figure 3a-b). Then, we observed decreases in α-SMA and Collagen I mRNA and protein levels after Nestin knockdown (figure 3c-f). Furthermore, knockdown of Nestin suppressed Smad2 phosphorylation and nuclear translocation (figure 3g-i and supplementary figure S3a-d). To further confirm the overall influences of Nestin on TGF-β pathway, we knocked out Nestin in human foetal lung fibroblast cell line (MRC-5) as reported in our previous study [12]. Consistent with the above results, TGF-β mediated phosphorylated Smad2 and α-SMA expression were markedly decreased (supplementary figure S3e-j). We also investigated the effect of Nestin on the activities of non-Smad TGF-β pathways through using luciferase reporters and found no significant differences in these pathways after Nestin knockdown (supplementary figure S4a-d). There were no marked changes in other effectors, such as Cav1 and Akt phosphorylation and β-catenin translocation, except Pai-1 (supplementary figure S4e-i). Taken together, these results revealed that Nestin deficiency primarily inhibits the TGF-β/Smad signalling pathway in vitro.

Nestin knockdown inhibits TGF-β signaling by regulating the stability of TβRI

TGF-β signalling is a canonical pathway that involves the phosphorylation of Smad by TGF-β receptor I (TβRI) and TGF-β receptor II (TβRII). Given that TGF-β receptors have been widely reported to significantly regulate the activation of the intracellular TGF-β signalling pathway [18-20], we assessed whether Nestin regulated the expression of TGF-β receptors and found that Nestin knockdown decreased the protein levels of TβRI instead of the mRNA levels of TβRI or TβRII in primary mouse lung fibroblasts and MRC5 (figure 4a-c and supplementary figure S5a-c). Furthermore, we tested the effect of Nestin knockdown on TβRI at different time points after TGF-β stimulation and found no differences with or without TGF-β stimulation (figure 4d-e). Accordingly, we treated primary mouse lung fibroblasts with the protein synthesis inhibitor, cycloheximide (CHX) and detected that Nestin knockdown resulted in a shortened half-life of TβRI (figure 4f-g). These data suggested that Nestin may modulate the stability of TβRI at the posttranslational level independent of TGF-β stimulation. Furthermore, the Nestin knockdown-induced inhibition of TGF-β-mediated Smad2 phosphorylation and nuclear translocation was completely restored by the reintroduction of TβRI (figure 4h-j and supplementary figure S5d). We also found that Nestin knockdown suppressed the TGF-β-mediated upregulation of α-SMA and Collagen I, and this effect could be rescued by overexpression of TβRI (figure 4k-m). These data suggested that Nestin knockdown inhibits TGF-β signalling and myofibroblast activation by inducing downregulation of TβRI expression.

Nestin knockdown inhibits the recycling of TβRI to the cell surface

Since TβRI is known to be endocytosed and recycled to the cell surface (figure 5a) and intracellular trafficking of TβRI is known to be required for TGF-β signalling [18], we first used biotinylation of cell-surface proteins to determine whether Nestin affected TβRI protein levels on the plasma membrane. Interestingly, the protein level of TβRI on the cell surface was decreased in Nestin-knockdown cells (figure 5b-c). Similarly, this result was further confirmed by flow cytometry (figure 5d-e). Endosomal receptors follow two trafficking routes in cells: some are recycled to the plasma membrane, while others are sorted to late endosomes/lysosomes for degradation [21, 23]. Accordingly, we used biotinylation assays to examine plasma membrane TβRI, TβRI endocytosis and TβRI recycling and found that only 50% of internalized TβRI was recycled in Nestin-knockdown cells compared to 75% in control cells (figure 5f-i). On the other hand, we also found that Nestin knockdown significantly increased the amount of TβRI that reached $LAMP1^+$ or $LAMP2^+$ vesicles (figure 5j-k). Moreover, knockdown of Nestin destabilized TβRI in primary mouse lung fibroblasts, which could be partially rescued by the lysosome inhibitor, chloroquine (Chlq) (figure 5l-n). Together, the above data indicated that Nestin knockdown may suppress TβRI recycling.

Nestin overexpression promotes TGF-β/Smad signaling and the recycling of TβRI

To further confirm the impact of Nestin on TβRI expression, recycling and signalling, we overexpressed Flag-Nestin in primary mouse lung fibroblasts (supplementary figure S6a). Consistently, Nestin overexpression increased the protein levels of TβRI

instead of the mRNA levels of TβRI or TβRII, and the TGFβ-inducible SBEs luciferase activities accordingly increased (supplementary figure S6b-e). Overexpression of Nestin promoted phosphorylated Smad2 nuclear translocation and upregulated the mRNA and protein levels of α-SMA and Collagen I (supplementary figure S6f-i). Furthermore, the protein level of surface TβRI was increased in Nestin-overexpressed cells (supplementary figure S6j-k), and Nestin overexpression significantly enhanced TβRI recycling to the cell surface, but showed no apparent effects on TβRI internalization (supplementary figure S6l-o).

Rab11 is required for the ability of Nestin to promote the recycling of TβRI to the cell surface

Recycling of TβRI to the plasma membrane is known to depend on Rab-like GTPases [25]. Rab4 and Rab11 play key roles in regulating the transport of cargo from early and late recycling endosomes to the cell surface, respectively [22-25]. Accordingly, we found that Nestin could colocalize with Rab11 but not Rab4 in primary mouse lung fibroblasts (figure 6a-c). Moreover, Nestin knockdown inhibited Rab11 GTPase activity (figure 6d-e). Furthermore, IF and co-IP showed that TβRI colocalized less with Rab11 in Nestin-knockdown cells (figure 6f-i). Thus, Nestin knockdown appears to inhibit the Rab11-dependent transportation of TβRI-containing recycling endosomes. We then investigated whether Rab11 was involved in Nestin-mediated TβRI recycling and found that TβRI in Nestin-knockdown cells colocalized less with $Rab11^{+}$ recycling vesicles but more with lysosomes, which could be partly rescued by overexpression of Rab11 (figure 6j-k and supplementary figure S7a-c). Meanwhile, the suppression of TGF-β mediated Smad2 phosphorylation and nuclear translocation by Nestin knockdown could be blocked by Rab11 overexpression (supplementary

figure S7d-f). Similarly, the inhibition of α-SMA and Collagen I upregulation in Nestin-knockdown cells after TGF-β stimulation was also rescued by reintroducing Rab11 (supplementary figure S7g-i). Taken together, these data suggested that Rab11 plays a critical role in Nestin-mediated recycling of TβRI to the plasma membrane.

Downregulation of Nestin attenuates pulmonary fibrosis in multiple experimental mice models

To examine the role of Nestin in the pathogenesis of pulmonary fibrosis in vivo, we subjected C57/BL6 mice to bleomycin or PBS injection and then intratracheally delivered AAV6-Scramble or AAV6-ShNES to the mice 10 days later (figure 7a). At 11 days after AAV6 delivery, we harvested lung tissues for analysis and found that both Nestin, Collagen I and α-SMA expression and Smad2 phosphorylation in lung tissues from the AAV6-ShNES group were significantly lower than in lung tissues from the AAV6-Scramble group (figure 7b-g). Consistently, the administration of AAV6-ShNES could attenuate bleomycin-induced pulmonary fibrosis, which was evidenced by hydroxyproline assays, H&E and Masson trichrome staining (figure 7h and supplementary figure S8a). Furthermore, knockdown of Nestin dramatically downregulated the bleomycin-induced expression of surface TβRI and α-SMA (supplementary figure S8b-d). Together, these data suggested that Nestin knockdown attenuated bleomycin-induced pulmonary fibrosis in vivo, and similar effects were observed in mouse 3D-lung tissue model and amiodarone-induced pulmonary fibrosis mouse model (supplementary figure S8e-m and S9a-h). We also made a non-inflammatory lung fibrosis model by administration of adenovirus containing TGF-β1 cDNA (figure 7i-j and supplementary figure S10a). Consistently, Collagen I

and α-SMA levels in lungs of AAV6-ShNES group were decreased compared with those of AAV6-Scramble group in AdTGF-β1 treated mice and Nestin knockdown inhibited TGF-β/Smad signaling pathway, which indicated the function of Nestin in pulmonary fibrosis may be dependent on TGF-β/Smad signaling rather than inflammation (figure 7k and supplementary figure S10b-l). Besides the therapeutic role of Nestin knockdown in bleomycin-induced pulmonary fibrosis, pretreated with AAV6-ShNES prior to bleomycin instillation further demonstrated the preventive effects of Nestin knockdown on bleomycin-induced pulmonary fibrosis (supplementary figure S11a-l and supplementary figure S12a-e).

Downregulation of Nestin inhibits TGF-β/Smad signaling pathway in human fibroblasts and pulmospheres

Furthermore, in order to demonstrate the potential of Nestin in a human background, we separated fibroblasts from human lung tissues and treated with Nestin expression interference [32]. The results showed that Nestin knockdown not only inhibited the expression of Collagen I and α-SMA, but also decreased TβRI expression and suppressed Smad2 phosphorylation and nuclear translocation in human fibroblasts with TGF-β treatment (figure 8a-j). Moreover, to clarify the therapeutic potential role of Nestin inhibition in human fibrosis model, we obtained human pulmospheres from normal and IPF lung biopsies (figure 8k). We observed decrease in α-SMA levels after Nestin knockdown in IPF pulmospheres (figure 8l-n). These data further confirmed that Nestin played a critical role in regulating TGF-β/Smad signaling pathway in a human background.

Discussion

IPF is a deadly disease with a high prevalence and affects 1 million people worldwide, and its management remains an ongoing challenge because of its complex and undefined aetiology [5]. Recent results indicate that Nestin expression is induced during fibrosis development in multiple organs, suggesting that this protein might be involved in the development of organ fibrosis [13, 33, 34]. Here, we provide evidence showing that Nestin regulates the vesicular trafficking system by promoting recycling of TβRI to the cell membrane through Rab11 and thereby contributes to the progression of pulmonary fibrosis (supplementary figure S13). More importantly, precise targeting of Nestin expression within lung myofibroblasts can alleviate lung fibrogenesis and may represent a potential therapeutic strategy for IPF.

Nestin is an intermediate filament protein. While it is widely known as a marker of neural stem cells, it is also expressed in the mesenchymal parts of various organs during the development and wound repair [8, 9]. Previous studies identified Nestin$^+$ fibroblasts in rat lungs, and a subpopulation exhibited a myofibroblast phenotype delineated by co-expression of smooth muscle α-actin, indicating they play a role in facilitating the reactive fibrotic response [33]. In an asthmatic Nestin-Cre; ROSA26-EYFP mouse model, Ke X et al. observed that Nestin$^+$ cells could differentiate into fibroblasts/myofibroblasts through RhoA/ROCK signalling activation [35]. In this study, we found that the Nestin level primarily increased in α-SMA$^+$ myofibroblasts in the lungs of IPF patients and bleomycin-treated mice, which resulted in collagen deposition and pulmonary fibrosis, similar to observations in previous studies. On the other hand, we also found that several Nestin$^+$ cells co-expressed pericyte marker (NG2$^+$) or smooth muscle cell marker (Calponin 1$^+$), with an increase of the absolute number of Nestin+NG2+ and Nestin+Calponin 1+

cells although the percentage of these two cell types decreased in lung fibrosis. Using a pulmonary hypertension Nestin-GFP mouse model, Saboor F et al. reported that Nestin-expressing pulmonary vascular smooth muscle cells drive the development of pulmonary hypertension [36]. Moreover, $NG2^+$ pericytes also accumulate and produce collagen near the fibrotic tissue in the lungs after injury, which leads to scar formation [37]. Considering that $Nestin^+NG2^+$ or $Nestin^+Calponin\ 1^+$ cells might also participate in the pathogenesis of pulmonary fibrosis, it will be interesting to further characterize the heterogeneity of $Nestin^+$ cells in lung fibrosis via single-cell sequencing and lineage tracing tools in the future.

The TGF-β/Smad family pathway plays a critical role in the activation of myofibroblasts and the progression of pulmonary fibrosis [17]. Many studies have demonstrated that endocytosis, intracellular trafficking and recycling of TGF-β receptors take part in TGF-β downstream signalling [23]. Clathrin-mediated and caveolae-mediated endocytosis are the two major pathways participating in the internalization of TGF-β receptors [19, 38]. Internalization of TGF-β receptors via clathrin-coated pits can enhance TGF-β signalling [18], whereas caveolae-mediated endocytosis of TGF-β receptors facilitates receptor degradation and thus the turnoff of signalling [39]. In this study, we demonstrated that Nestin is a central regulator of the intracellular vesicular trafficking system and promotes the recycling of TβRI to the cell membrane via Rab11. However, we did not observe significant changes on caveolin-1 protein expression after Nestin knockdown in primary mouse lung fibroblasts (supplementary figure S4f-g), which indicates that Nestin might not be mainly involved in caveolae-mediated endocytosis of TβRI in pulmonary fibrosis. Because the clathrin-mediated pathway also participates in internalization and transportation of TGF-β receptors to early endosomes [40], whether Nestin regulates TGF-β receptors

endocytosis and recycling through the clathrin-mediated pathway needs to be clarified in future studies.

Although the TGF-β/Smad signalling pathway is one of the drivers of organ fibrosis progression, TGF-β receptor inhibitors might not be suitable for treating pulmonary fibrosis [41], because TGF-β receptors are widely distributed in various cell types and participate in the pleiotropic functions including cellular proliferation, differentiation and migration [42]. Therefore, more precise cellular and molecular targets are urgently needed. Recently, AAV vectors have come to be regarded as an effective and relatively safe gene delivery tool in clinical trials, due to their low oncogenicity and weak immunogenicity [43, 44]. In the present study, we injected AAV6 vectors intratracheally to knock down Nestin in the lungs of mice and found that the efficacy of AAV6 transduction in α-SMA$^+$ myofibroblasts was approximately 80%, indicating a relatively high targeting effect of AAV6-ShNES on lung myofibroblasts. Compared with the AAV6-Scramble group, those subjected to AAV6-mediated Nestin knockdown exhibited dramatic attenuation of pulmonary fibrosis, as indicated by the alleviation of collagen accumulation and improvement of histopathological alterations. Further exploration of the therapeutic effects of targeting Nestin in lung fibrosis will be of interest.

There are also several limitations in our study. Firstly, Nestin mRNA abundance was different from its protein expression, probably because firstly, there might exist multiple processes beyond transcript concentration contributing to establishing the expression level of a protein [45]; secondly, there existed different types of protein-mRNA correlations [46]; and what's more, this might be due to the sc-RNA-seq sensitivity, which limited the detection for some transcripts in a large proportion of cells [47, 48].

Besides, myofibroblasts are a group of heterogenous cells, which are the major source of accumulated extracellular matrix during organ fibrosis [49], and the origin of these cells may come from multiple cell types such as proliferating lung resident fibroblasts [50]; $CD73^+$ and $Pdgfrb1^+$ pericytes [51]; $Gli1^+$ mesenchymal stromal cells [52]; dysfunctional epithelial cells [53]. Meanwhile, as for the regulation and cell-type expression of Nestin in normal and fibrotic lungs, it was demonstrated that Nestin was expressed heterogeneously in various cell populations in lungs such as fibroblasts/myofibroblasts or pulmonary vascular smooth muscle cells [33, 35, 36]. In our study, we found that Nestin mainly expressed in myofibroblasts and some expressed in pericytes and smooth muscle cells in normal and fibrotic lungs. Therefore, lineage tracing experiments will need to be performed to determine whether $Nestin^+$ cells can serve as the origin of lung myofibroblasts in vivo in future studies.

Acknowledgements

We thank the Core Facility of Center, Zhongshan School of Medicine, Sun Yat-Sen University for providing instruments for two-photon fluorescence microscopy and a Zeiss 880 Laser Scanning Confocal Microscope with Airyscan.

Support statement: the National Key Research and Development Program of China, Stem cell and Translational Research (2018YFA0107200, 2017YFA0103403, 2017YFA0103802) Strategic Priority Research Program of the Chinese Academy of Sciences (XDA16010103, XDA16020701) the National Natural Science Foundation of China (81730005, 31771616, 81802402, 81971372) the Key Research and Development Program of Guangdong Province (2016B030229002, 2017B020231001, 2019B020234001, 2019B020236002, 2019B020235002) Key Scientific and Technological Program of Guangzhou City (201803040011, 201704020223) the Fundamental Research Funds for the Central Universities (19ykpy158) and the Research Start-up Fund of the Seventh Affiliated Hospital, Sun Yat-sen University (393011).

References

1. Sheppard D. ROCKing pulmonary fibrosis. *J Clin Invest* 2013: 123(3): 1005-1006.
2. Travis WD, Costabel U, Hansell DM, King TE, Jr., Lynch DA, Nicholson AG, Ryerson CJ, Ryu JH, Selman M, Wells AU, Behr J, Bouros D, Brown KK, Colby TV, Collard HR, Cordeiro CR, Cottin V, Crestani B, Drent M, Dudden RF, Egan J, Flaherty K, Hogaboam C, Inoue Y, Johkoh T, Kim DS, Kitaichi M, Loyd J, Martinez FJ, Myers J, Protzko S, Raghu G, Richeldi L, Sverzellati N, Swigris J, Valeyre D, Pneumonias AECoII. An official American Thoracic Society/European Respiratory Society statement: Update of the international multidisciplinary classification of the idiopathic interstitial pneumonias. *Am J Respir Crit Care Med* 2013: 188(6): 733-748.
3. Raghu G, Weycker D, Edelsberg J, Bradford WZ, Oster G. Incidence and prevalence of idiopathic pulmonary fibrosis. *Am J Respir Crit Care Med* 2006: 174(7): 810-816.
4. Ahluwalia N, Shea BS, Tager AM. New therapeutic targets in idiopathic pulmonary fibrosis. Aiming to rein in runaway wound-healing responses. *Am J Respir Crit Care Med* 2014: 190(8): 867-878.
5. Selman M, King TE, Pardo A, American Thoracic S, European Respiratory S, American College of Chest P. Idiopathic pulmonary fibrosis: prevailing and evolving hypotheses about its pathogenesis and implications for therapy. *Ann Intern Med* 2001: 134(2): 136-151.
6. Lendahl U, Zimmerman LB, McKay RD. CNS stem cells express a new class of intermediate filament protein. *Cell* 1990: 60(4): 585-595.
7. Cattaneo E, McKay R. Proliferation and differentiation of neuronal stem cells regulated by nerve growth factor. *Nature* 1990: 347(6295): 762-765.
8. Mendez-Ferrer S, Michurina TV, Ferraro F, Mazloom AR, Macarthur BD, Lira SA, Scadden DT, Ma'ayan A, Enikolopov GN, Frenette PS. Mesenchymal and haematopoietic stem cells form a unique bone marrow niche. *Nature* 2010: 466(7308): 829-834.
9. Jiang MH, Cai B, Tuo Y, Wang J, Zang ZJ, Tu X, Gao Y, Su Z, Li W, Li G, Zhang M, Jiao J, Wan Z, Deng C, Lahn BT, Xiang AP. Characterization of Nestin-positive stem Leydig cells as a potential source for the treatment of testicular Leydig cell dysfunction. *Cell research* 2014: 24(12): 1466-1485.
10. Wang J, Cai J, Huang Y, Ke Q, Wu B, Wang S, Han X, Wang T, Wang Y, Li W, Lao C, Song W, Xiang AP. Nestin regulates proliferation and invasion of gastrointestinal stromal tumor cells by altering mitochondrial dynamics. *Oncogene* 2016: 35(24): 3139-3150.
11. Wang J, Lu Q, Cai J, Wang Y, Lai X, Qiu Y, Huang Y, Ke Q, Zhang Y, Guan Y, Wu H, Wang Y, Liu X, Shi Y, Zhang K, Wang M, Peng Xiang A. Nestin regulates cellular redox homeostasis in lung cancer through the Keap1-Nrf2 feedback loop. *Nature communications* 2019: 10(1): 5043.
12. Zhang Y, Wang J, Huang W, Cai J, Ba J, Wang Y, Ke Q, Huang Y, Liu X, Qiu Y, Lu Q, Sui X, Shi Y, Wang T, Shen H, Guan Y, Zhou Y, Chen Y, Wang M, Xiang AP. Nuclear Nestin deficiency drives tumor senescence via lamin A/C-dependent nuclear deformation. *Nature communications* 2018: 9(1): 3613.
13. Niki T, Pekny M, Hellemans K, Bleser PD, Berg KV, Vaeyens F, Quartier E, Schuit F, Geerts A. Class VI intermediate filament protein nestin is induced during activation of rat hepatic stellate cells. *Hepatology (Baltimore, Md)* 1999: 29(2): 520-527.

14. Tomioka M, Hiromura K, Sakairi T, Takeuchi S, Maeshima A, Kaneko Y, Kuroiwa T, Takeuchi T, Nojima Y. Nestin is a novel marker for renal tubulointerstitial injury in immunoglobulin A nephropathy. *Nephrology (Carlton)* 2010: 15(5): 568-574.
15. Beguin PC, Gosselin H, Mamarbachi M, Calderone A. Nestin expression is lost in ventricular fibroblasts during postnatal development of the rat heart and re-expressed in scar myofibroblasts. *Journal of cellular physiology* 2012: 227(2): 813-820.
16. Correction: Role of Transforming Growth Factor (beta) in Human Disease. *N Engl J Med* 2000: 343(3): 228.
17. Fernandez IE, Eickelberg O. The impact of TGF-beta on lung fibrosis: from targeting to biomarkers. *Proc Am Thorac Soc* 2012: 9(3): 111-116.
18. Di Guglielmo GM, Le Roy C, Goodfellow AF, Wrana JL. Distinct endocytic pathways regulate TGF-beta receptor signalling and turnover. *Nat Cell Biol* 2003: 5(5): 410-421.
19. Chen YG. Endocytic regulation of TGF-beta signaling. *Cell research* 2009: 19(1): 58-70.
20. Li M, Krishnaveni MS, Li C, Zhou B, Xing Y, Banfalvi A, Li A, Lombardi V, Akbari O, Borok Z, Minoo P. Epithelium-specific deletion of TGF-beta receptor type II protects mice from bleomycin-induced pulmonary fibrosis. *J Clin Invest* 2011: 121(1): 277-287.
21. Rahimi RA, Leof EB. TGF-beta signaling: a tale of two responses. *J Cell Biochem* 2007: 102(3): 593-608.
22. Butterworth MB, Edinger RS, Silvis MR, Gallo LI, Liang X, Apodaca G, Frizzell RA, Johnson JP. Rab11b regulates the trafficking and recycling of the epithelial sodium channel (ENaC). *Am J Physiol Renal Physiol* 2012: 302(5): F581-590.
23. Grant BD, Donaldson JG. Pathways and mechanisms of endocytic recycling. *Nat Rev Mol Cell Biol* 2009: 10(9): 597-608.
24. Takahashi S, Kubo K, Waguri S, Yabashi A, Shin HW, Katoh Y, Nakayama K. Rab11 regulates exocytosis of recycling vesicles at the plasma membrane. *J Cell Sci* 2012: 125(Pt 17): 4049-4057.
25. Mitchell H, Choudhury A, Pagano RE, Leof EB. Ligand-dependent and -independent transforming growth factor-beta receptor recycling regulated by clathrin-mediated endocytosis and Rab11. *Mol Biol Cell* 2004: 15(9): 4166-4178.
26. Jiang MH, Li G, Liu J, Liu L, Wu B, Huang W, He W, Deng C, Wang D, Li C, Lahn BT, Shi C, Xiang AP. Nestin(+) kidney resident mesenchymal stem cells for the treatment of acute kidney ischemia injury. *Biomaterials* 2015: 50: 56-66.
27. Liu RM, Vayalil PK, Ballinger C, Dickinson DA, Huang WT, Wang S, Kavanagh TJ, Matthews QL, Postlethwait EM. Transforming growth factor beta suppresses glutamate-cysteine ligase gene expression and induces oxidative stress in a lung fibrosis model. *Free Radic Biol Med* 2012: 53(3): 554-563.
28. Xie N, Tan Z, Banerjee S, Cui H, Ge J, Liu RM, Bernard K, Thannickal VJ, Liu G. Glycolytic Reprogramming in Myofibroblast Differentiation and Lung Fibrosis. *Am J Respir Crit Care Med* 2015: 192(12): 1462-1474.
29. Shichino S, Ueha S, Hashimoto S, Otsuji M, Abe J, Tsukui T, Deshimaru S, Nakajima T, Kosugi-Kanaya M, Shand FH, Inagaki Y, Shimano H, Matsushima K. Transcriptome network analysis identifies protective role of the LXR/SREBP-1c axis in murine pulmonary fibrosis. *JCI Insight* 2019: 4(1).
30. Tsukui T, Sun KH, Wetter JB, Wilson-Kanamori JR, Hazelwood LA, Henderson NC, Adams TS, Schupp JC, Poli SD, Rosas IO, Kaminski N, Matthay MA, Wolters PJ, Sheppard D. Collagen-producing lung cell atlas identifies multiple subsets with distinct localization and relevance to fibrosis. *Nat Commun* 2020: 11(1): 1920.

31. McDonough JE, Ahangari F, Li Q, Jain S, Verleden SE, Herazo-Maya J, Vukmirovic M, DeIuliis G, Tzouvelekis A, Tanabe N, Chu F, Yan X, Verschakelen J, Homer RJ, Manatakis DV, Zhang J, Ding J, Maes K, De Sadeleer L, Vos R, Neyrinck A, Benos PV, Bar-Joseph Z, Tantin D, Hogg JC, Vanaudenaerde BM, Wuyts WA, Kaminski N. Transcriptional regulatory model of fibrosis progression in the human lung. *JCI Insight* 2019: 4(22).
32. Bueno M, Lai YC, Romero Y, Brands J, St Croix CM, Kamga C, Corey C, Herazo-Maya JD, Sembrat J, Lee JS, Duncan SR, Rojas M, Shiva S, Chu CT, Mora AL. PINK1 deficiency impairs mitochondrial homeostasis and promotes lung fibrosis. *J Clin Invest* 2015: 125(2): 521-538.
33. Chabot A, Meus MA, Naud P, Hertig V, Dupuis J, Villeneuve L, El Khoury N, Fiset C, Nattel S, Jasmin JF, Calderone A. Nestin is a marker of lung remodeling secondary to myocardial infarction and type I diabetes in the rat. *J Cell Physiol* 2015: 230(1): 170-179.
34. Sakairi T, Hiromura K, Yamashita S, Takeuchi S, Tomioka M, Ideura H, Maeshima A, Kaneko Y, Kuroiwa T, Nangaku M, Takeuchi T, Nojima Y. Nestin expression in the kidney with an obstructed ureter. *Kidney Int* 2007: 72(3): 307-318.
35. Ke X, Do DC, Li C, Zhao Y, Kollarik M, Fu Q, Wan M, Gao P. Ras homolog family member A/Rho-associated protein kinase 1 signaling modulates lineage commitment of mesenchymal stem cells in asthmatic patients through lymphoid enhancer-binding factor 1. *J Allergy Clin Immunol* 2019: 143(4): 1560-1574 e1566.
36. Saboor F, Reckmann AN, Tomczyk CU, Peters DM, Weissmann N, Kaschtanow A, Schermuly RT, Michurina TV, Enikolopov G, Muller D, Mietens A, Middendorff R. Nestin-expressing vascular wall cells drive development of pulmonary hypertension. *Eur Respir J* 2016: 47(3): 876-888.
37. Birbrair A, Zhang T, Files DC, Mannava S, Smith T, Wang ZM, Messi ML, Mintz A, Delbono O. Type-1 pericytes accumulate after tissue injury and produce collagen in an organ-dependent manner. *Stem Cell Res Ther* 2014: 5(6): 122.
38. Doherty GJ, McMahon HT. Mechanisms of endocytosis. *Annu Rev Biochem* 2009: 78: 857-902.
39. Hayes S, Chawla A, Corvera S. TGF beta receptor internalization into EEA1-enriched early endosomes: role in signaling to Smad2. *J Cell Biol* 2002: 158(7): 1239-1249.
40. Takei K, Haucke V. Clathrin-mediated endocytosis: membrane factors pull the trigger. *Trends Cell Biol* 2001: 11(9): 385-391.
41. Akhurst RJ, Hata A. Targeting the TGFbeta signalling pathway in disease. *Nat Rev Drug Discov* 2012: 11(10): 790-811.
42. Hata A, Chen YG. TGF-beta Signaling from Receptors to Smads. *Cold Spring Harbor perspectives in biology* 2016: 8(9).
43. Crystal RG. Adenovirus: the first effective in vivo gene delivery vector. *Hum Gene Ther* 2014: 25(1): 3-11.
44. Li H, Malani N, Hamilton SR, Schlachterman A, Bussadori G, Edmonson SE, Shah R, Arruda VR, Mingozzi F, Wright JF, Bushman FD, High KA. Assessing the potential for AAV vector genotoxicity in a murine model. *Blood* 2011: 117(12): 3311-3319.
45. McManus J, Cheng Z, Vogel C. Next-generation analysis of gene expression regulation--comparing the roles of synthesis and degradation. *Mol Biosyst* 2015: 11(10): 2680-2689.
46. Liu Y, Beyer A, Aebersold R. On the Dependency of Cellular Protein Levels on mRNA Abundance. *Cell* 2016: 165(3): 535-550.

47. Ziegenhain C, Vieth B, Parekh S, Reinius B, Guillaumet-Adkins A, Smets M, Leonhardt H, Heyn H, Hellmann I, Enard W. Comparative Analysis of Single-Cell RNA Sequencing Methods. *Mol Cell* 2017: 65(4): 631-643 e634.
48. Svensson V, Natarajan KN, Ly LH, Miragaia RJ, Labalette C, Macaulay IC, Cvejic A, Teichmann SA. Power analysis of single-cell RNA-sequencing experiments. *Nat Methods* 2017: 14(4): 381-387.
49. Hinz B, Phan SH, Thannickal VJ, Prunotto M, Desmouliere A, Varga J, De Wever O, Mareel M, Gabbiani G. Recent developments in myofibroblast biology: paradigms for connective tissue remodeling. *Am J Pathol* 2012: 180(4): 1340-1355.
50. Rosas IO, Kottmann RM, Sime PJ. New light is shed on the enigmatic origin of the lung myofibroblast. *Am J Respir Crit Care Med* 2013: 188(7): 765-766.
51. Hung C, Linn G, Chow YH, Kobayashi A, Mittelsteadt K, Altemeier WA, Gharib SA, Schnapp LM, Duffield JS. Role of lung pericytes and resident fibroblasts in the pathogenesis of pulmonary fibrosis. *Am J Respir Crit Care Med* 2013: 188(7): 820-830.
52. Cassandras M, Wang C, Kathiriya J, Tsukui T, Matatia P, Matthay M, Wolters P, Molofsky A, Sheppard D, Chapman H, Peng T. Gli1(+) mesenchymal stromal cells form a pathological niche to promote airway progenitor metaplasia in the fibrotic lung. *Nat Cell Biol* 2020: 22(11): 1295-1306.
53. Auyeung VC, Sheppard D. Stuck in a Moment: Does Abnormal Persistence of Epithelial Progenitors Drive Pulmonary Fibrosis? *Am J Respir Crit Care Med* 2021: 203(6): 667-669.

Figure Legends:

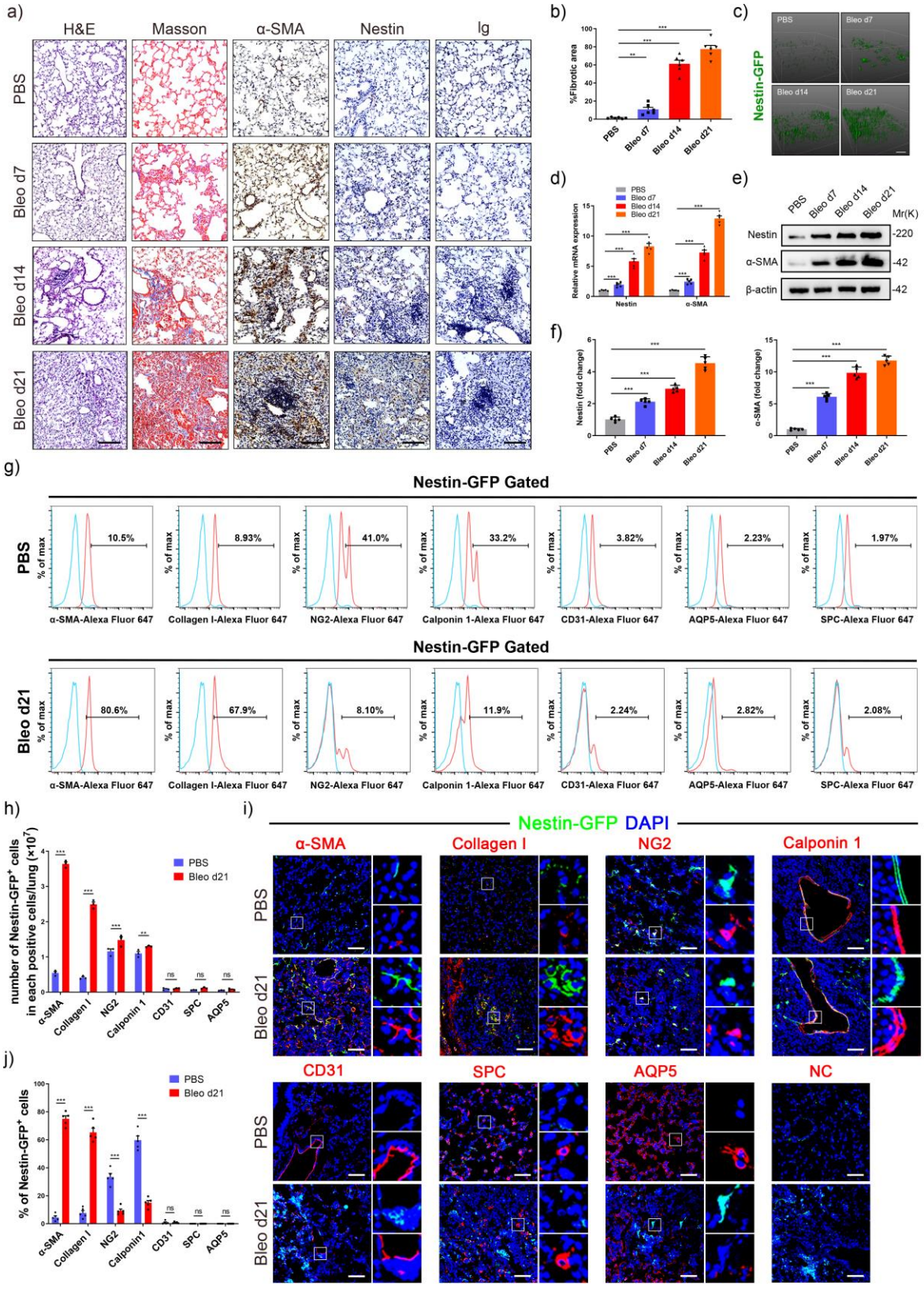

Figure 1: Nestin is upregulated in experimental pulmonary fibrosis, and localized mainly in lung myofibroblasts.

a) H&E staining, Masson's trichrome staining and immunohistochemistry images obtained using anti-α-SMA, anti-Nestin antibody of lung sections from C57/BL6 mice on day 7, 14 and 21 days after bleomycin exposure (n=6 per group). b) Quantification of the area occupied by fibrotic stroma in the Masson's trichrome staining results presented in a) (n=6 per group). c) Two-photon fluorescent images of lung sections obtained from Nestin-GFP mice (n=6 per group). Scale bars: 100 μm. d) qPCR analysis of α-SMA and Nestin mRNA expression levels in lungs on 7, 14 and 21 days after bleomycin exposure (n=5 mice per group). e) Western blot analysis and f) quantification of Nestin and α-SMA expression in lungs on 7, 14 and 21 days after bleomycin exposure (n=5 mice per group). g) Flow cytometry was carried out to determine the co-expression of Nestin and α-SMA and Collagen I (myofibroblasts), NG2 (pericytes), Calponin 1 (smooth muscle cells), CD31 (vascular endothelial cells), SPC (type II alveolar epithelial cells), or AQP5 (type I alveolar epithelial cells) respectively in mice control and fibrotic lung samples. h) Statistical analysis of the number of Nestin-positive cells in each positive cell type, as obtained from g), (n=3 mice per group). i) Immunofluorescence was carried out to determine the co-localization of Nestin-GFP (green) and α-SMA (myofibroblasts), Collagen I (myofibroblasts), NG2 (pericytes), Calponin 1 (smooth muscle cells), CD31 (vascular endothelial cells), SPC (type II alveolar epithelial cells) or AQP5 (type I alveolar epithelial cells) (red) in lungs. Scale bars: 50 μm. j) Semiquantitative scoring of double-positive cells as a percentage of Nestin-positive cells, as obtained from immunofluorescent images (n=5 mice per group; five fields assessed per sample).

Data are presented as the mean ± SD; *P<0.05, **P<0.01, ***P<0.001; One-way ANOVA and Tukey’s multiple comparisons test.

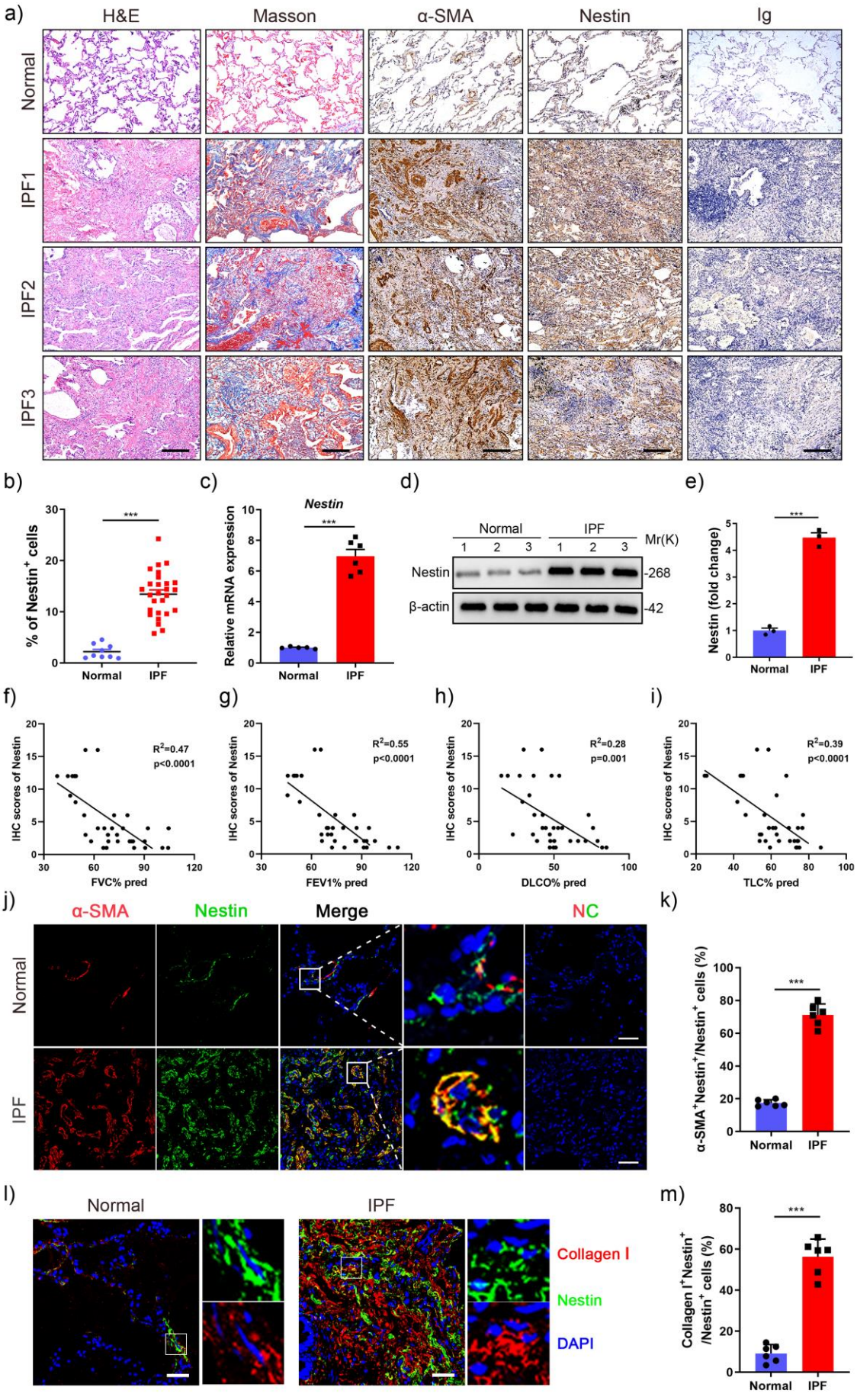
a)
H&E
Masson
α-SMA
Nestin
Ig
Normal
IPF1
IPF2
IPF3
b)
% of Nestin+ cells
***
Normal
IPF
c)
Nestin
Relative mRNA expression
***
Normal
IPF
d)
Normal
IPF
1 2 3 1 2 3
Mr(K)
Nestin
-268
β-actin
-42
e)
Nestin (fold change)
***
Normal
IPF
f)
IHC scores of Nestin
R2=0.47
p<0.0001
FVC% pred
g)
IHC scores of Nestin
R2=0.55
p<0.0001
FEV1% pred
h)
IHC scores of Nestin
R2=0.28
p=0.001
DLCO% pred
i)
IHC scores of Nestin
R2=0.39
p<0.0001
TLC% pred
j)
α-SMA
Nestin
Merge
NC
Normal
IPF
k)
α-SMA+Nestin+/Nestin+ cells (%)
***
Normal
IPF
l)
Normal
IPF
Collagen I
Nestin
DAPI
m)
Collagen I+Nestin+ /Nestin+ cells (%)
***
Normal
IPF

Figure 2: Nestin is upregulated in the lungs of patients with idiopathic pulmonary fibrosis.

a) H&E staining, Masson's trichrome staining, immunohistochemistry images of α-SMA and Nestin in lung sections from IPF patients and healthy donors. Scale bars: 200 µm. b) Quantification of Nestin-positive cells of immunohistochemistry images from IPF patients and healthy donors (n=27 IPF patients, n=9 healthy donors; five fields assessed per sample). c) qPCR analysis of Nestin mRNA expression in the lungs from IPF patients and healthy donors. (n=6 IPF patients, n=5 healthy donors). d) Western blot analysis and e) quantification of Nestin expression in lung sections from IPF patients and healthy donors. (n=3 IPF patients, n=3 healthy donors). Linear regression between Nestin expression in patients with IPF and clinical parameters such as f) FVC% pred, g) FEV1% pred, h) DLCO% pred and i) TLC% pred (n=35 IPF patients). j) Immunofluorescence staining of Nestin and α-SMA in lung sections from IPF patients and healthy donors. k) Semiquantitative scoring of double-positive cells as a percentage of Nestin-positive cells, as obtained from immunofluorescent images (n=6 IPF patients, n=6 healthy donors; five fields assessed per sample). Scale bars: 50 µm. l) Immunofluorescence staining of lung tissues from normal and IPF patients visualized using anti-Nestin (green) and anti-Collagen I (red). Scale bars: 50 µm. m) Semiquantitative scoring of double-positive cells as a percentage of Nestin-positive cells, as obtained from immunofluorescent images (n=6 IPF patients, n=6 healthy donors; five fields assessed per sample). Data are presented as the mean ± SD of three independent experiments; *P<0.05, **P<0.01, ***P<0.001; One-way ANOVA and Tukey's multiple comparisons test.

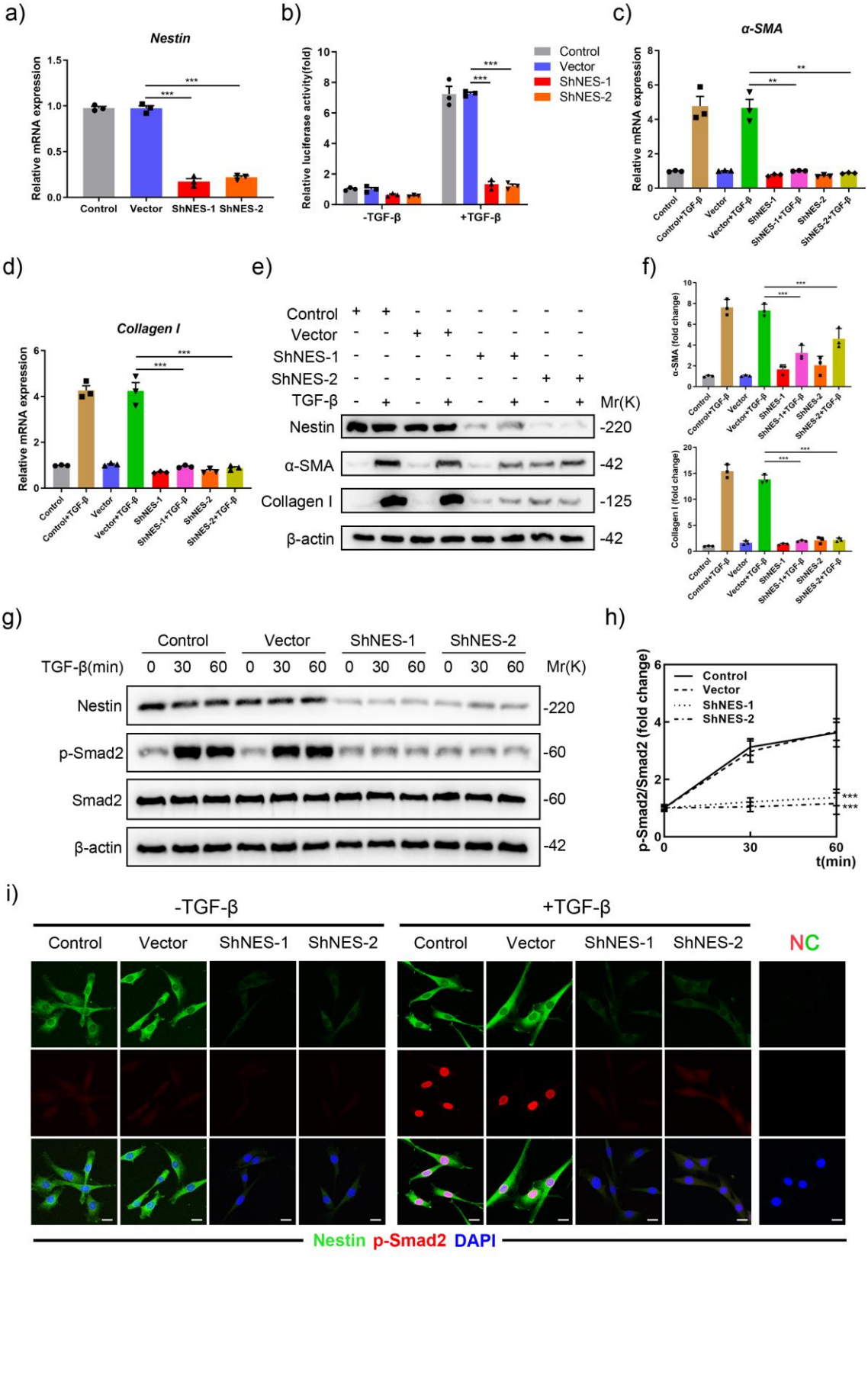
a)
Nestin
Relative mRNA expression
Control
Vector
ShNES-1
ShNES-2
b)
Relative luciferase activity(fold)
-TGF-β
+TGF-β
c)
α-SMA
Relative mRNA expression
d)
Collagen I
e)
Mr(K)
Nestin
α-SMA
Collagen I
β-actin
f)
α-SMA (fold change)
Collagen I (fold change)
g)
TGF-β(min)
p-Smad2
Smad2
h)
p-Smad2/Smad2 (fold change)
t(min)
i)
NC
Nestin p-Smad2 DAPI

Figure 3: Nestin knockdown inhibits TGF-β/Smad signaling.

a) Nestin expression in primary mouse lung fibroblasts was analyzed by qPCR (n=3 per group). b) Nestin-knockdown primary mouse lung fibroblasts were transfected with pGL3-SBE9-luciferase constructs and treated with or without TGF-β (5 ng/ml) for 24 hours, and luciferase activity was measured (n=3 per group). c) qPCR analysis of α-SMA mRNA expression in primary mouse lung fibroblasts with Nestin knockdown (n=3 per group). d) qPCR analysis of Collagen I mRNA expression in primary mouse lung fibroblasts with Nestin knockdown (n=3 per group). e) Western blot analysis and f) quantification of α-SMA and Collagen I expression in Nestin-knockdown primary mouse lung fibroblasts treated for 72 hours with or without TGF-β (5 ng/ml) (n=3 per group). g) Western blot analysis and h) quantification of p-Smad2 and Smad2 expression in Nestin-knockdown primary mouse lung fibroblasts treated with or without TGF-β (5 ng/ml) (n=3 per group). i) Immunofluorescence staining of Nestin-knockdown primary mouse lung fibroblasts treated with or without TGF-β (5 ng/ml) and visualized using anti-Nestin (green) and anti-p-Smad2 (red). Scale bars: 10 μm. Data are presented as the mean ± SD of three independent experiments; **P*<0.05, ***P*<0.01, ****P*<0.001; One-way ANOVA and Tukey's multiple comparisons test.

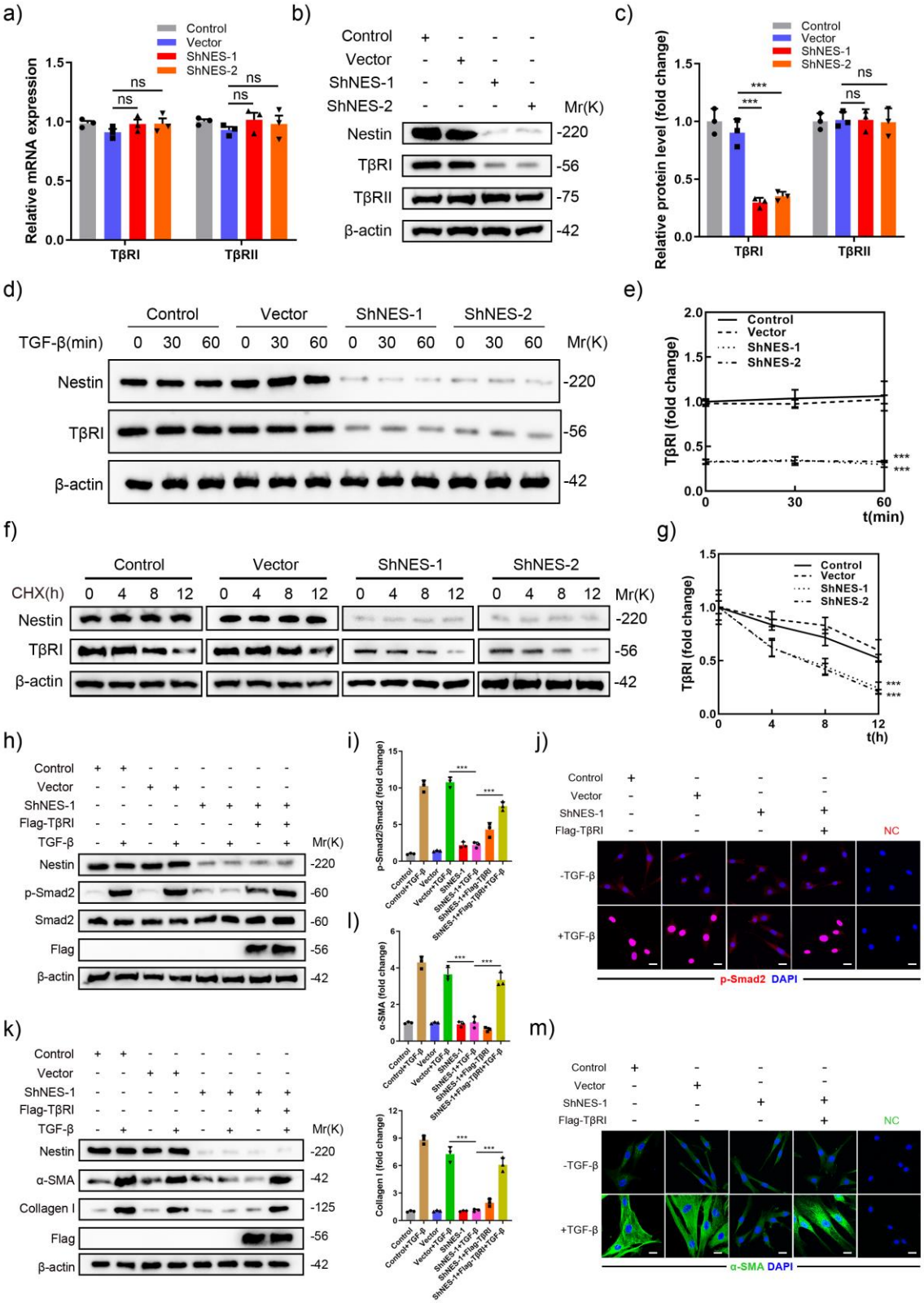

Figure 4: Nestin knockdown inhibits TGF-β/Smad signaling via regulating the stability of TβRI in mice.

a) qPCR analysis of TβRI and TβRII mRNA expression levels in Nestin-knockdown primary mouse lung fibroblasts (n=3 per group). b) Western blot analysis and c) quantification of TβRI and TβRII expression in Nestin-knockdown primary mouse lung fibroblasts (n=3 per group). d) Western blot analysis and e) quantification of TβRI expression in Nestin-knockdown primary mouse lung fibroblasts at different time points after TGF-β (5 ng/ml) stimulation (n=3 per group). f) Half-life analysis and g) quantification of TβRI in Nestin-knockdown primary mouse lung fibroblasts. All cell groups were treated with cycloheximide (CHX, 50 μg/ml) harvested at the indicated times (0, 4, 8, 12 hours after CHX treated) and subjected to immunoblotting (n=3 per group). h) Western blot analysis and i) quantification of Smad2 phosphorylation levels with Nestin knockdown and TβRI overexpression treated with or without TGF-β (5 ng/ml) (n=3 per group). j) Immunofluorescence staining of p-Smad2 in primary mouse lung fibroblasts by Nestin knockdown and overexpression of TβRI. Scale bars: 20 μm. k) Western blot analysis and l) quantification of α-SMA and Collagen I expression levels in primary mouse lung fibroblasts by Nestin knockdown and overexpression of TβRI (n=3 per group). m) Immunofluorescence staining of α-SMA in primary mouse lung fibroblasts by Nestin knockdown and overexpression of TβRI. Scale bars: 20 μm. Data are presented as the mean ± SD of three independent experiments; **P*<0.05, ***P*<0.01, ****P*<0.001; One-way ANOVA and Tukey's multiple comparisons test.

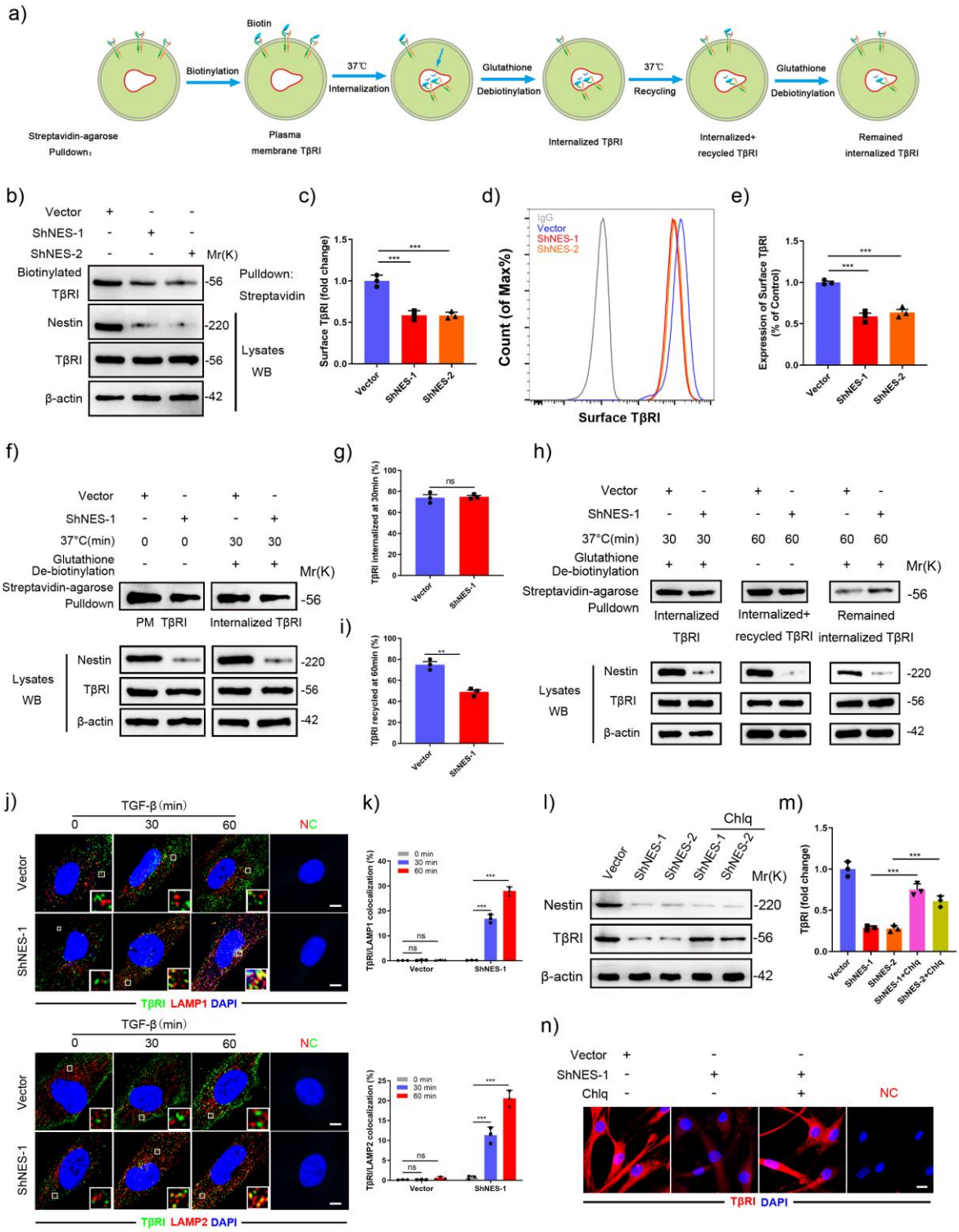
a)
Biotin
Biotinylation
37℃
Internalization
Glutathione
Debiotinylation
37℃
Recycling
Glutathione
Debiotinylation
Streptavidin-agarose
Pulldown:
Plasma
membrane TβRI
Internalized TβRI
Internalized+
recycled TβRI
Remained
internalized TβRI
b)
Vector
ShNES-1
ShNES-2
Mr(K)
Biotinylated
TβRI
Pulldown:
Streptavidin
Nestin
TβRI
β-actin
Lysates
WB
-56
-220
-56
-42
c)
Surface TβRI (fold change)
Vector
ShNES-1
ShNES-2
d)
IgG
Vector
ShNES-1
ShNES-2
Count (of Max%)
Surface TβRI
e)
Expression of Surface TβRI
(% of Control)
f)
37°C(min)
Glutathione
De-biotinylation
Streptavidin-agarose
Pulldown
PM TβRI
Internalized TβRI
g)
TβRI internalized at 30min (%)
ns
h)
Internalized
TβRI
Internalized+
recycled TβRI
Remained
internalized TβRI
i)
TβRI recycled at 60min (%)
j)
TGF-β (min)
0
30
60
NC
TβRI LAMP1 DAPI
TβRI LAMP2 DAPI
k)
TβRI/LAMP1 colocalization (%)
TβRI/LAMP2 colocalization (%)
0 min
30 min
60 min
l)
Chlq
Nestin
TβRI
β-actin
m)
TβRI (fold change)
ShNES-1+Chlq
ShNES-2+Chlq
n)
TβRI DAPI

Figure 5: Nestin knockdown inhibits the recycling of TβRI to the cell surface.

a) Schematic overview of the biotinylation assay for quantifying plasma membrane TβRI level, TβRI endocytosis and recycling. b) Detect the protein levels of TβRI on the plasma membrane in biotinylated serum-starved Nestin-knockdown primary mouse lung fibroblasts after treated with chloroquine (Chlq,100μM) for 4h. c) quantification of surface TβRI protein levels in b) (n=3 per group). d) Live-cell FACS analysis of surface TβRI levels in Nestin-knockdown primary mouse lung fibroblasts. e) Quantification of TβRI levels shown in panel d) (n=3 per group). f) Biotinylated serum-starved Nestin-knockdown primary mouse lung fibroblasts were placed at 37°C for 30 min and then treated with glutathione after treated with Chlq (100μM) for 4h, and subjected to streptavidin agarose pull down and western blot analysis of TβRI, g) Quantification of the percentage of internalized TβRI in f) (n=3 per group); TβRI internalization rate = total internalized TβRI at 30 min / Plasma membrane TβRI × 100%. h) Western blot analysis of recycled TβRI at 60 min. i) Quantification of the percentage of recycled TβRI in h) (n=3 per group); TβRI recycling rate = (internalized and recycled TβRI at 60 min – internalized TβRI at 60 min) / total internalized TβRI at 30 min × 100%). j) Immunofluorescence staining of LAMP1 or LAMP2 and TβRI in Nestin-knockdown primary mouse lung fibroblasts treated with TGF-β (5 ng/ml). Scale bars: 5 μm. k) Quantification of the percentage of TβRI co-localized with LAMP1 or LAMP2. (n=3; five fields assessed per sample). l) Western blot analysis and m) quantification of TβRI expression levels in Nestin-knockdown primary mouse lung fibroblasts treated with or without Chlq (100μM) (n=3 per group). n) Immunofluorescence staining of TβRI in Nestin-knockdown primary mouse lung fibroblasts treated with or without Chlq (100μM) for 4h. Scale bars: 20 μm. Data are

presented as the mean ± SD of three independent experiments; *P<0.05, **P<0.01, ***P<0.001; Unpaired t test and one-way ANOVA and Tukey's multiple comparisons test. PM: plasma membrane.

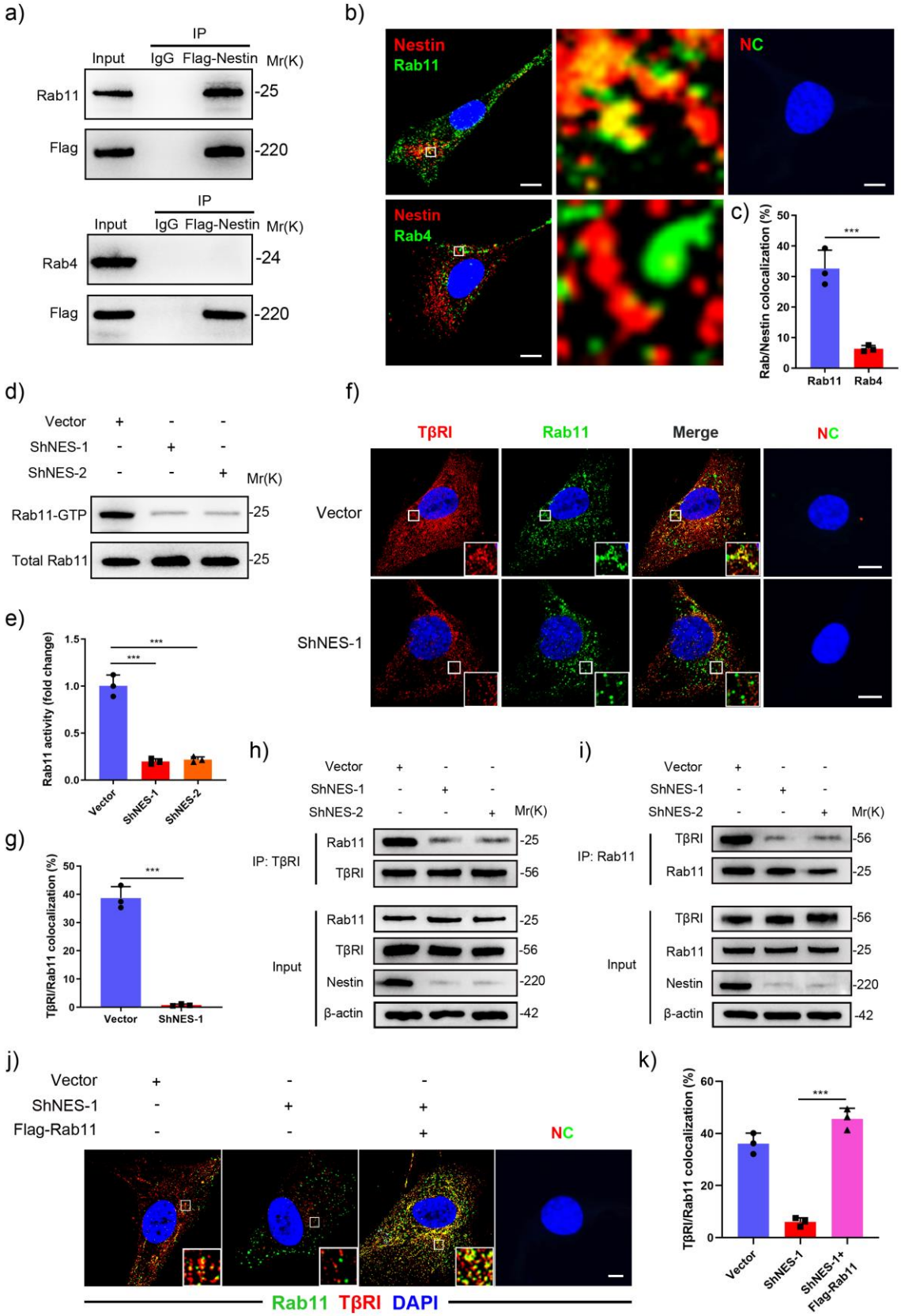
a)
IP
Input
IgG
Flag-Nestin
Mr(K)
Rab11
-25
Flag
-220
IP
Input
IgG
Flag-Nestin
Mr(K)
Rab4
-24
Flag
-220
b)
Nestin
Rab11
NC
Nestin
Rab4
c)
Rab/Nestin colocalization (%)
***
Rab11
Rab4
d)
Vector + - -
ShNES-1 - + -
ShNES-2 - - +
Mr(K)
Rab11-GTP
-25
Total Rab11
-25
e)
Rab11 activity (fold change)
***
***
Vector
ShNES-1
ShNES-2
f)
TβRI
Rab11
Merge
NC
Vector
ShNES-1
g)
TβRI/Rab11 colocalization (%)
***
Vector
ShNES-1
h)
Vector + - -
ShNES-1 - + -
ShNES-2 - - +
Mr(K)
IP: TβRI
Rab11
-25
TβRI
-56
Input
Rab11
-25
TβRI
-56
Nestin
-220
β-actin
-42
i)
Vector + - -
ShNES-1 - + -
ShNES-2 - - +
Mr(K)
IP: Rab11
TβRI
-56
Rab11
-25
Input
TβRI
-56
Rab11
-25
Nestin
-220
β-actin
-42
j)
Vector + - -
ShNES-1 - + +
Flag-Rab11 - - +
NC
Rab11 TβRI DAPI
k)
TβRI/Rab11 colocalization (%)
***
Vector
ShNES-1
ShNES-1+ Flag-Rab11

Figure 6: Rab11 is required for the ability of Nestin to promote the recycling of TβRI to the cell surface.

a) Immunoprecipitation was performed using an anti-Flag-Nestin antibody, and immunoblotting of the protein levels of Rab11 and Rab4 in Nestin-knockdown primary mouse lung fibroblasts. b) Immunofluorescence staining showed the colocalization between Nestin and Rab11, Rab4 in primary mouse lung fibroblasts. Scale bars: 10 μm. c) Quantification of the percentage of Nestin co-localized with Rab11 and Rab4 (n=3; five fields assessed per sample). d) Rab11 activity assays were performed in Nestin-knockdown primary mouse lung fibroblasts. e) quantification of Rab11GTPase activity (n=3 per group). f) Immunofluorescence staining of Rab11 and TβRI in Nestin-knockdown primary mouse lung fibroblasts. Scale bars: 5 μm. g) Quantification of the percentage of TβRI co-localized with Rab11. (n=3; five fields assessed per sample). h) Immunoprecipitation was performed using an anti-TβRI antibody, and immunoblotting of the protein levels of Rab11 in Nestin-knockdown primary mouse lung fibroblasts treated with Chlq (100μM) for 4h. i) Immunoprecipitation was performed using an anti-Rab11 antibody, and immunoblotting of the protein levels of TβRI in Nestin-knockdown primary mouse lung fibroblasts treated with Chlq (100μM) for 4h. j) Immunofluorescence staining of TβRI and Rab11 in Nestin-knockdown primary mouse lung fibroblasts with overexpression of Rab11. Scale bars: 5 μm. k) Quantification of the percentage of TβRI co-localized with Rab11. (n=3; five fields assessed per sample). Scale bars: 5 μm. Data are presented as the mean ± SD of three independent experiments; **P*<0.05, ***P*<0.01, ****P*<0.001; Unpaired *t* test and one-way ANOVA and Tukey's multiple comparisons test.

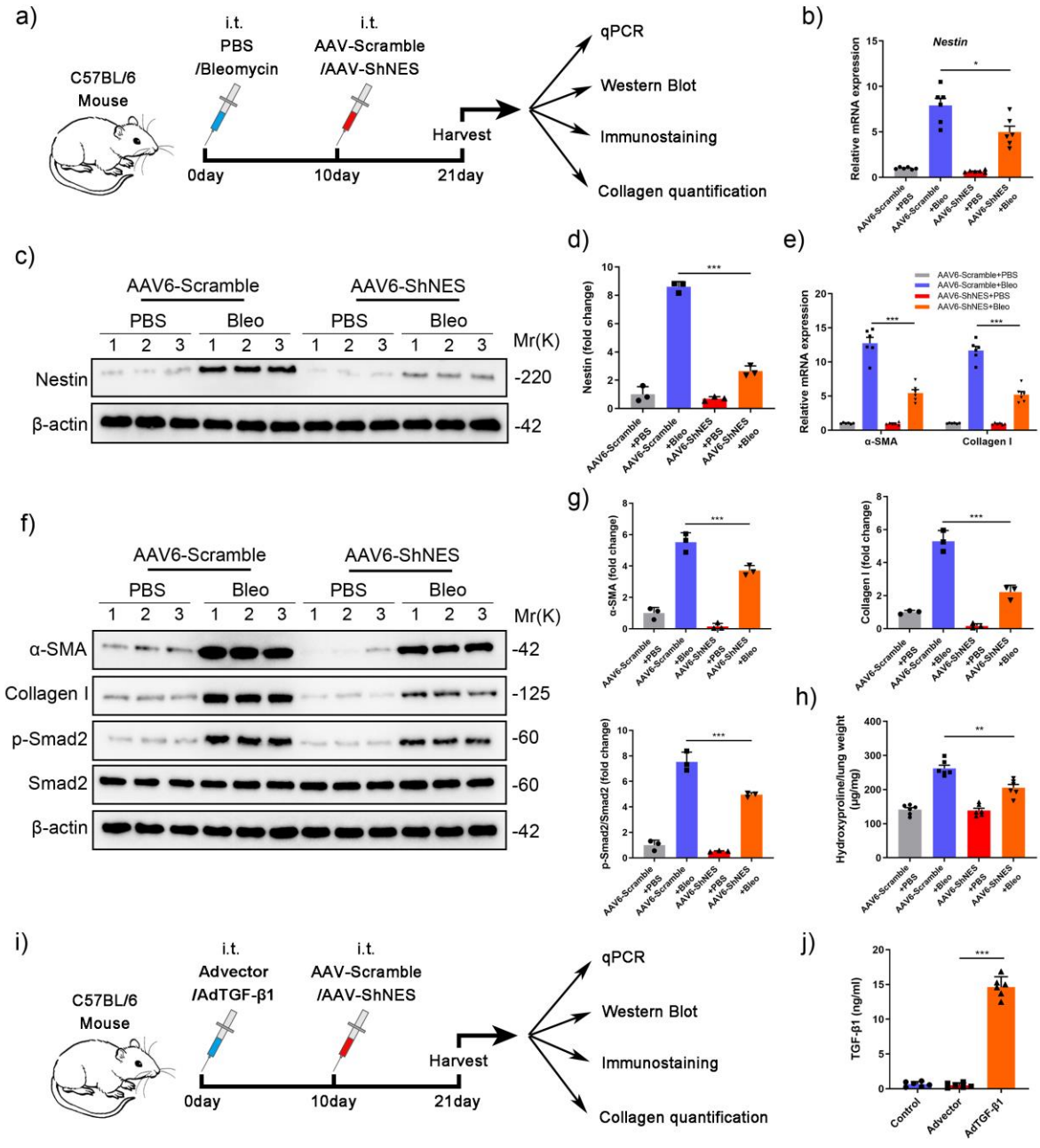
a)
C57BL/6
Mouse
i.t.
PBS
/Bleomycin
i.t.
AAV-Scramble
/AAV-ShNES
0day
10day
Harvest
21day
qPCR
Western Blot
Immunostaining
Collagen quantification
b)
Nestin
Relative mRNA expression
AAV6-Scramble +PBS
AAV6-Scramble +Bleo
AAV6-ShNES +PBS
AAV6-ShNES +Bleo
c)
AAV6-Scramble
AAV6-ShNES
PBS
Bleo
Mr(K)
Nestin
β-actin
-220
-42
d)
Nestin (fold change)
e)
Relative mRNA expression
α-SMA
Collagen I
f)
α-SMA
Collagen I
p-Smad2
Smad2
β-actin
-42
-125
-60
-60
-42
g)
α-SMA (fold change)
Collagen I (fold change)
p-Smad2/Smad2 (fold change)
h)
Hydroxyproline/lung weight (μg/mg)
i)
C57BL/6
Mouse
i.t.
Advector
/AdTGF-β1
i.t.
AAV-Scramble
/AAV-ShNES
0day
10day
Harvest
21day
qPCR
Western Blot
Immunostaining
Collagen quantification
j)
TGF-β1 (ng/ml)
Control
Advector
AdTGF-β1
k)
Nestin
α-SMA
Merge
Nestin
TβRI
Merge
Nestin
p-Smad2
Merge
NC
AAV6-Scramble
Advector
AdTGF-β1
AAV6-ShNES
Advector
AdTGF-β1

Figure 7: Downregulation of Nestin attenuates bleomycin-induced pulmonary fibrosis and TGF-β overexpression-induced pulmonary fibrosis in mice.

a) Experimental design. 8-week-old C57BL/6 mice were intratracheally injected with bleomycin (3U/kg) or PBS. Ten days later, the mice were intratracheally injected with AAV6-ShNES or AAV6-Scramble. Samples were collected for analysis 21 days after bleomycin administration. b) qPCR analysis of Nestin mRNA expression in the lungs of C57/BL6 mice from the different groups (n=6 mice per group). c) Western blot analysis and d) quantification of Nestin expression levels in lungs from C57/BL6 mice of the different groups (n=3 per group). e) qPCR analysis of α-SMA and Collagen I mRNA expression levels in lungs from C57/BL6 mice of the different groups (n=6 mice per group). f) Western blot analysis and g) quantification of α-SMA, Collagen I, p-Smad2 and Smad2 expression levels in lungs from C57/BL6 mice of the different groups (n=3 per group). h) Hydroxyproline levels in lungs of C57/BL6 mice from the different groups (n=6 mice per group). i) Experimental design. 8-week-old C57BL/6 mice were intratracheally injected with AdTGF-β1 or Advector. Ten days later, the mice were intratracheally injected with AAV6-ShNES or AAV6-Scramble. Samples were collected for analysis 21 days after bleomycin administration. j) TGF-β1 levels in the lungs of C57/BL6 mice from the different groups (n=6 mice per group). k) Immunofluorescence staining with Nestin, α-SMA, TβRI and p-Smad2 in lung slices from the different groups. Scale bars: 70 μm. Data are presented as the mean ± SD of three independent experiments; **P*<0.05, ***P*<0.01, ****P*<0.001; One-way ANOVA and Tukey's multiple comparisons test.

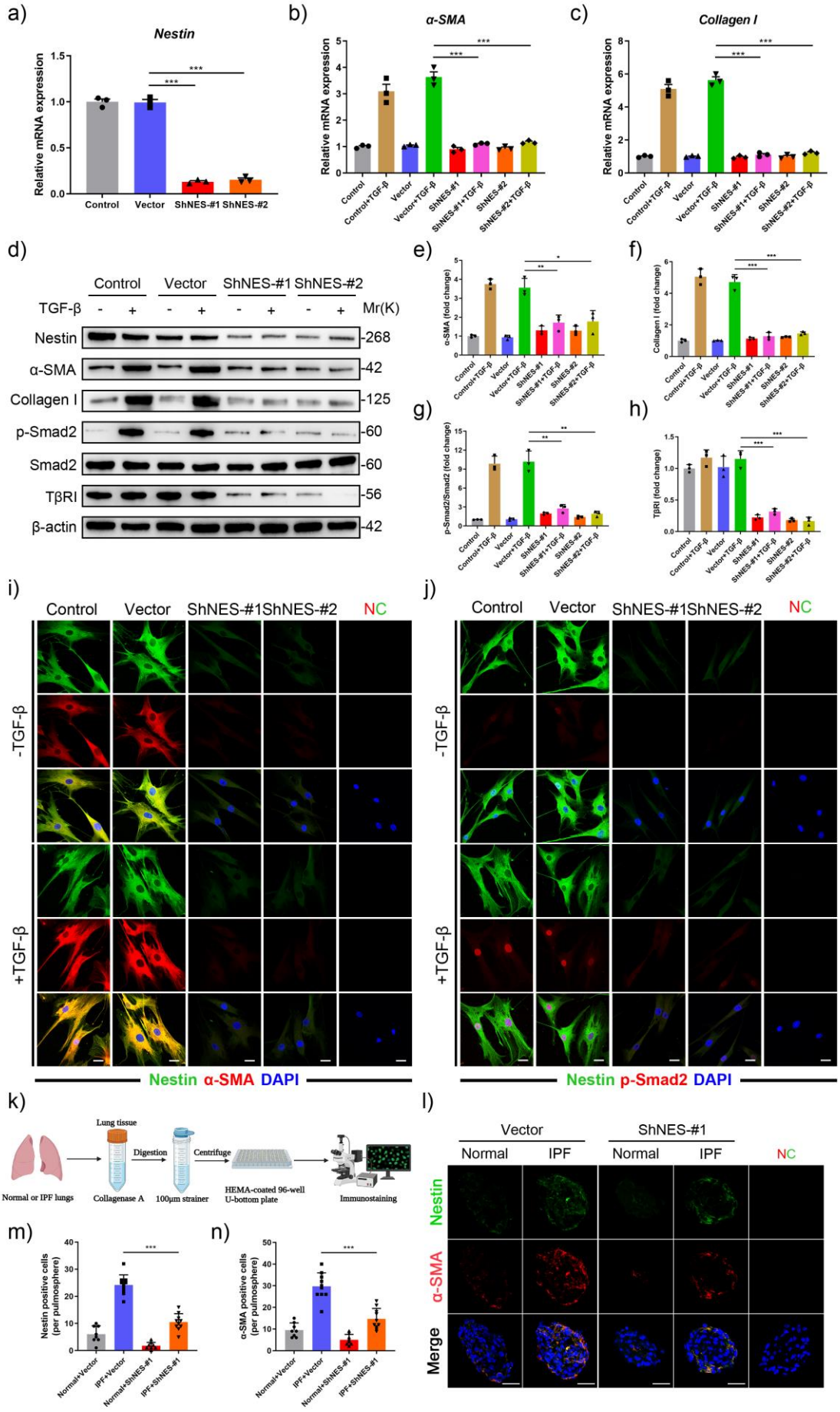
a)
Nestin
Relative mRNA expression
Control
Vector
ShNES-#1
ShNES-#2
b)
α-SMA
c)
Collagen I
Control+TGF-β
Vector+TGF-β
ShNES-#1+TGF-β
ShNES-#2+TGF-β
d)
Control
Vector
ShNES-#1
ShNES-#2
TGF-β
Mr(K)
Nestin
α-SMA
Collagen I
p-Smad2
Smad2
TβRI
β-actin
-268
-42
-125
-60
-60
-56
-42
e)
α-SMA (fold change)
f)
Collagen I (fold change)
g)
p-Smad2/Smad2 (fold change)
h)
TβRI (fold change)
i)
Control
Vector
ShNES-#1
ShNES-#2
NC
-TGF-β
+TGF-β
Nestin α-SMA DAPI
j)
Nestin p-Smad2 DAPI
k)
Lung tissue
Digestion
Centrifuge
Normal or IPF lungs
Collagenase A
100μm strainer
HEMA-coated 96-well U-bottom plate
Immunostaining
l)
Vector
ShNES-#1
Normal
IPF
NC
Nestin
α-SMA
Merge
m)
Nestin positive cells (per pulmosphere)
Normal+Vector
IPF+Vector
Normal+ShNES-#1
IPF+ShNES-#1
n)
α-SMA positive cells (per pulmosphere)

Figure 8: Nestin knockdown inhibits TGF-β/Smad signaling in human fibroblasts and pulmospheres.

a) Nestin expression in primary human lung fibroblasts was analyzed by qPCR (n=3 per group). b) qPCR analysis of α-SMA mRNA expression in human lung fibroblasts with Nestin knockdown (n=3 per group). c) qPCR analysis of Collagen I mRNA expression in human lung fibroblasts with Nestin knockdown (n=3 per group). d) Western blot analysis and quantification of e) α-SMA, f) Collagen I, g) p-smad2, smad2 and h) TβRI expression in Nestin-knockdown human lung fibroblasts treated for 72 hours with or without TGF-β (5 ng/ml) (n=3 per group). i) Immunofluorescence staining of Nestin-knockdown human lung fibroblasts treated with or without TGF-β (5 ng/ml) and visualized using anti-Nestin (green) and anti-α-SMA (red). Scale bars: 10 µm. j) Immunofluorescence staining of Nestin-knockdown human lung fibroblasts treated with or without TGF-β (5 ng/ml) and visualized using anti-Nestin (green) and anti-p-Smad2 (red). Scale bars: 10 µm. k) Overview of human pulmospheres preparation from normal and IPF lung tissues and immunostaining. l) Immunofluorescence staining of Nestin-knockdown human pulmospheres and visualized using anti-Nestin (green) and anti-α-SMA (red). Scale bars: 50 µm. m) Quantification of Nestin positive cells per pulmosphere in l). n) Quantification of α-SMA positive cells per pulmosphere in l). Data are presented as the mean ± SD of three independent experiments; *P<0.05, **P<0.01, ***P<0.001; One-way ANOVA and Tukey's multiple comparisons test.

Supplementary material and methods

Cell isolation and culture

Primary mouse and human lung fibroblast isolation were performed as previously described [1, 2]. Fresh lungs from 12-weeks old normal mice or normal human lung tissues were perfused, isolated under sterile conditions and excised into nearly 1-mm^3 fragments, which were then digested in DMEM supplemented with 10 mg/ml dispase (Sigma-Aldrich, D4693) and 20 mg/ml Collagenase type I (Gibco, Thermo Fisher Scientific, 9001-12-1) at 37°C for 2 hours and then sequentially filtered through 100-μm, 40-μm and 15-μm pore filters to remove undigested tissues. Single cells were washed to remove the enzyme and maintained for 1 week in DMEM supplemented with 10% fetal bovine serum (FBS, Gibco) and penicillin-streptomycin. The cells were then cultured in a humidified atmosphere of 5% CO_2 at 37°C as described previously to allow fibroblasts to grow and become the dominant cell type [3, 4]. Outgrowing fibroblasts were reached confluence and passaged by trypsinization. Cultured fibroblasts were used for experiments at passages 3 to 6. Identification of fibroblasts was based on the expression of vimentin, collagen I, and α-SMA. Human fetal pulmonary fibroblasts (MRC5 cells) and HEK293T cells were purchased from American Type Culture Collection (ATCC).

Vectors and reagents

For loss of Nestin function, retrovirus vectors (pSM2) encoding Nestin shRNA were used as previously described [5]. Scramble shRNA served as a control. All shRNAs were constructed in our laboratory. Details on the plasmids are provided in Supplemental Table 3. ShRNA transfections were performed using the MegaTran 1.0 Transfection Reagent (OriGene) according to the manufacturer's instructions. For Nestin overexpression, Full-length Nestin were cloned into pcDNA3.1-Myc vector (Invitrogen). Myc-Nestin vector was constructed using Invitrogen's Gateway System. The pcDNA3.1-Myc served as the empty control vector. Flag-tagged TβR Ⅰ, Nestin and Rab11 were constructed using Invitrogen's Gateway System. TGF-β, CHX and Chloroquine (Chlq) were purchased from Sigma-Aldrich.

Generation of murine 3D-LTCs and AAV6 treatment

3D-LTCs from C57BL/6 mice and bleomycin-induced pulmonary fibrosis mice model were performed as previously described [6, 7]. The procedure was performed under sterile conditions. Control and bleomycin-induced pulmonary fibrosis mice were anaesthetised with isoflurane. After intubation and dissection of the diaphragm, lungs were flushed via the heart with sterile sodium chloride solution. Using a syringe pump, lungs were infiltrated with warm, low gelling temperature agarose (2%, A9414; Sigma; kept at 40°C) in sterile cultivation medium (DMEM/Ham's F12; Gibco, supplemented with 100

$U \cdot mL^{-1}$ penicillin, 100 $\mu g \cdot mL^{-1}$ streptomycin and 2.5 $\mu g \cdot mL^{-1}$ amphotericin B; Sigma). The trachea was ligated with thread to retain the agarose inside the lung. The lung was excised, transferred into a tube with cultivation medium and cooled on ice for 10 min to allow gelling of the agarose. The lobes were separated and cut with a vibratome (VT1200s, Leica, Germany) to a thickness of 300 µm using a speed of 10-12 $\mu m \cdot s^{-1}$, a frequency of 150 Hz and an amplitude of 1.2 mm. The 3D-LTCs were cultivated in medium supplemented with 0.1% fetal calf serum (FCS, Gibco). Individual 3D-LTCs were cultivated at 37°C in humidified conditions containing 5% (volume/ volume) CO_2 in 24-well plates under submerged conditions with changes of medium every other day. 3D-LTCs obtained from mice subjected to PBS or bleomycin were stimulated either with AAV6-Scramble or AAV6-ShNES ($1*10^{12}$vg/slice) for 72h.

Preparation of pulmospheres

Lung biopsies (approximately 6 mm × 6 mm) from IPF patients or control subjects were perfused, isolated under sterile conditions and excised into nearly 1-mm^3 fragments, washed with cold PBS solution. The tissue was then digested in DMEM supplemented with 20 mg/ml Collagenase type I (Gibco, Thermo Fisher Scientific, 9001-12-1) at 37°C for 1 hour. The tube containing tissue was then vigorously shaken for 1 min and the resulting suspension was filtered through a 100-µm strainer. The filtered cell suspension was centrifuged for 5 minutes at 300 g. The cell pellet was resuspended in DMEM and then

seeded into HEMA-coated (5 mg/ml made in 95% ethanol) 96-well U-bottom plates in complete culture medium consisting of DMEM supplemented with 10% fetal bovine serum (FBS, Gibco) and penicillin-streptomycin. The cells were cultured in a humidified atmosphere of 5% CO_2 at 37°C as described previously.

Real-time quantitative PCR

Total RNA was extracted from lung tissues or cells using the TRIzol reagent (Molecular Research Center, Inc.) following the manufacturer's protocol. Quantification was performed with a NanoDrop 8000 spectrophotometer and 1 μg of total RNA was used to reverse transcription with a RevertAid First Strand cDNA Synthesis Kit (Thermo Fisher Scientific, K1622). The obtained cDNAs were used as the template for real-time quantitative PCR (qPCR) reactions with the FastStart Essential DNA Green Master Mix (Roche, 06924204001). All samples were run in triplicate and the results were normalized to those obtained for the 18S rRNA or GAPDH. The primers designed and used for qPCR are described in Supplemental Table 4.

Histopathological evaluation

After sacrifice, mouse lung tissues were perfused with 4% paraformaldehyde and then subjected to paraffin embedding or saturation in 30% sucrose for 24 hours for frozen sections. Paraffin-embedded human IPF and mouse lung

tissue sections were exposed to H&E or Masson trichrome staining to analyze collagens and inflammation, respectively, in the lung tissue sections.

Immunohistochemistry (IHC) and Immunofluorescent staining (IF)

Paraffin-embedded human IPF and mouse lung tissue sections were subjected to immunostaining using an UltraSensitiveTM SP (Mouse/Rabbit) IHC Kit (MXB, KIT-9710). Following deparaffinization and antigen retrieval, the IPF lung tissue specimens were incubated overnight with corresponding antibodies listed in Supplemental Table 5. Signal amplification and detection were performed using a DAB system according to the manufacturer's instructions (MXB, MAX-001).

Immunofluorescent staining of human IPF and mouse lung tissue sections was performed using primary antibodies listed in Supplemental Table 5. Semi-quantitative analyses of Nestin staining were performed in mouse lungs using five non-overlapping tissue fields evaluated under ×20 magnification. Stained sections were imaged using a two-photon fluorescence microscopy (FVMPE-RS), a Zeiss 800 Laser Scanning Confocal Microscope, a Zeiss 880 Laser Scanning Confocal Microscope with Airyscan and Dragonfly CR-DFLY-202 2540 (Andor, UK). All mean fluorescence intensity of immunofluorescent staining results were analyzed with the Image J software (NIH).

Lung Tissue Dissociations

Single-cell suspensions of lung cells were prepared by mincing and enzymatic digestion. Briefly, lungs were rinsed in sterile phosphate-buffered saline (PBS) following removal of tracheas, and were finely minced with sterile scissors and incubated in 3 mg/ml collagenase type I (#17018029, ThermoFisher) (Diluted with HBSS, in supplement with 0.1% BSA) in a volume of 2 ml per lung for 60 minutes at 37°C in a shaking incubator. The resulting cell suspension was further filtered through a 40 μm sieve successively to avoid the cell aggregates, and washed twice in PBS supplemented with 1% FBS, 1 mM EDTA (#A100105, Sangon Biotech) by centrifugation (1,100 rpm, 5 minutes, room temperature).

Then, prior to the next step, all the tissues were washed (a 5-min centrifugation at 1100rpm, room temperature) twice with FACS buffer, which was PBS in supplemented with 1% FBS, 1 mM EDTA (#A100105, Sangon Biotech).

Flow Cytometric Assay

Single-cell suspensions of lung cells where stained using corresponding antibodies listed in Supplemental Table 5, thereafter fixed with 4% PFA, permeabilized using PBS buffer (0.1% saponin in PBS with 0.1% BSA) for 90min at room temperature. Cells were then stained with secondary antibody conjugated with Alexa Flour 647 in the dark for 45min on ice. Cells were then washed twice with FACS buffer and run on CytoFLEX (Beckman Coulter,

USA). Data were analyzed using the Flow Jo software (Tree Star Inc., Ashland, Oregon).

Quantification of cell surface TβRI using FACS analysis

The cells were seeded at 2×10^5 cells per well of six-well plates, harvested from plates and washed with FACS buffer (1% bovine serum albumin in PBS containing 0.5 mM EDTA) twice. Cells were stained with anti-mouse TβRI-APC antibody or rat IgG_{2A} APC isotype control and then incubated in the dark for 30 min (on ice). Cells were then washed twice with FACS buffer and run on CytoFLEX (Beckman Coulter, USA). Data were analyzed using the Flow Jo software (Tree Star Inc., Ashland, Oregon).

Adeno-associated virus (AAV) delivery

Two versions of adeno-associated virus vector serotype 6 expressing ShNES under the control of the human CMV promoter were purchased from the Hanbio Biotechnology Co., Ltd (Shanghai, China). C57BL/6 mice (8-week-old, male) were deeply anesthetized and intratracheally administered with 1.5×10^{12} viral genomes of a pseudotyped AAV6 GFP vector or 1.5×10^{12} viral genomes of a pseudotyped AAV6 Nestin vector.

Cell fractionation

Cytoplasmic and nuclear fractions were separated using a Nucleoprotein Extraction Kit (Sangon Biotech, C510001) according to the manufacturer's instructions. The nuclear pellet was resuspended in 20 mM Hepes (pH 7.9), 1 mM EGTA, 1 mM EDTA, 0.4 M NaCl, 1 mM dithiothreitol, and 1 mM phenylmethylsulfonyl fluoride. Purity of the fractions was assessed by western blot analysis of the obtained fractions. β-actin and Lamin B were marker proteins for the cytosolic extract and the nuclear extract respectively.

Immunoprecipitation and immunoblotting

p-Smad2, Collagen I, Nestin, Smad2, β-Actin, Flag, TβRI, TβRII, Rab11, Rab4, Lamin B, p-Akt, Akt, Cav1 protein expression in lung tissue samples and cells were measured by immunoblotting performed as previously described [5]. Antibodies are listed in Supplemental Table 5. Immunoprecipitation was assessed in cells using a previously described method [5]. Bands from at least three independent blots were quantified using Image J software.

Gene targeting by the CRISPR/Cas9 system

The plasimds used for CRISPR/Cas9 KO in MRC5 was constructed in our previous study according to the established cloning protocol [8, 9], and T7E1 assay was also performed for sgRNA screening as previously described [5].

MRC5 Transfection Kit (Altogen Biosystems, Catalog #2175) was used for introducing the control (Cas9-GFP) and Nestin-knockout (G2-Cas9-GFP) plasmids into the MRC5 cells. Three days after transfection, MRC5 cells were single cell sorted using an Influx Cell Sorter (BD, USA) into a plastic flat-bottomed 96 well plate, and allowed to expand. Approximately 27.56% of these clones survived and were initially screened for Nestin gene deletion by PCR amplicons from selected genomic region on a duplicated plate and subjected to 2% agarose gel electrophoresis. Clones with negative results were further validated for Nestin KO by a western blot and were then cultured and harvested for further experiments.

Luciferase reporter assays

The pGL3-SRE luciferase reporter (Cat. #11545ES03) and pGL3-ELK-1 luciferase reporter (Cat. #11567ES03) were purchased from Yeasen Biotechnology (Shanghai). The pGL3-FOXO luciferase reporter, pGL3-AP-1 luciferase reporter were generous gifts from Junchao Cai. The pGL3-(SBE)9-reporter and Renilla luciferase vectors were purchased from Promega and the assays were performed as described by the provided manual (Cat.# E1960). Briefly, cells were transiently co-transfected with the Renilla luciferase vector and the respective reporters. At 24 h post-transfection, the cells were starved for 20 h in culture medium with 1% FBS and then treated with TGF-β (5 ng/ml) or vehicle (0.1% BSA; 4 mM HCl)

for 24 h. The luciferase activity was analyzed using a Dual Luciferase Assay System (Promega). The luciferase data of the cells transfected with pGL3 Basic vectors were calculated and normalized with respect to the Renilla luciferase activity. All transfection was carried out in triplicate. All data were plotted as mean values obtained from triplicate determinations, with SDs.

Biotinylation assay for plasma membrane TβRI, TβRI endocytosis and TβRI recycling

All cells were first treated with chloroquine (Chlq) (100μM) for 4h and then were performed the following experiments.

To quantitate plasma membrane TβRI, cells were placed on ice, washed twice with ice-cold PBS, incubated with 0.2 mM biotin (Thermo Fisher Scientific) in PBS at 4°C for 30 min, and washed twice with 0.1 M glycine. Biotinylated proteins were pulled down with streptavidin agarose (S1638, Sigma-Aldrich) and immunoblotted for plasma membrane TβRI.

To quantitate endogenous TβRI endocytosis, cells were moved to 4°C and labeled with cleavable biotin. Two washes were performed with ice-cold PBS, and then the cells were resuspended in pre-warmed culture medium and incubated at 37°C to allow for TβRI endocytosis. Thirty minutes later, the cells were then returned to 4°C and washed once with ice-cold PBS to stop membrane trafficking. To strip the remaining biotin from the cell surface, cells were treated twice with stripping buffer (50 mM glutathione, 75 mM NaCl, 10

mM EDTA, 1% BSA, 0.075 N NaOH) at 4°C for 15 min. Cell lysates were then subjected to streptavidin agarose pull down and immunoblotted for TβRI.

To quantitate TβRI recycling at 37°C, cells were moved to 4°C, labeled with cleavable biotin and incubated for 30 or 60 min in a 37°C incubator. Cells were treated without stripping buffer (50 mM glutathione, 75 mM NaCl, 10 mM EDTA, 1% BSA, 0.075 N NaOH) and harvested at the end of incubation or subjected to two additional washes at 4°C for 15 min with stripping buffer (50 mM glutathione, 75 mM NaCl, 10 mM EDTA, 1% BSA, 0.075 N NaOH) to ensure the complete de-biotinylation of recycled TβRI. Cell lysates were subjected to streptavidin agarose pull down and analyzed by immunoblotting. All immunoblotting results were analyzed with the Image J software (NIH). In the lysates of cell incubated for 60 min without glutathione treatment, the biotinylated TβRI included the internalized and recycled TβRI. While in the lysates of cells incubated for 60 min with glutathione treatment, all of the biotinylated TβRI was remained internalized TβRI. The recycling rate of TβRI after 60 min of incubation was calculated by the following formula: TβRI recycling rate = (internalized and recycled TβRI at 60 min – internalized TβRI at 60 min) / total internalized TβRI at 30 min × 100% [10, 11].

Rab11 activity assay

Rab11 activity was determined using a Rab11 activity assay kit (NewEast Biosciences, King of Prussia, PA) according to the manufacturer's instructions.

Cell lysates containing Rab11-GTP were incubated with anti-active Rab11 mouse monoclonal antibody (Catalog No. 26919). The bound active Rab11 was pulled down with protein A/G agarose (Catalog No. 30301) and detected by immunoblotting using anti-Rab11 rabbit polyclonal antibody (Catalog No. 21157).

Hydroxyproline assay

Frozen lung tissue samples from mice were incubated in 250 µl PBS, after which 250 µl of 12 N HCl was added into samples for pellet hydrolysis at 110°C were overnight. Samples were neutralized by the addition of 10 N NaOH. 100 µl of each sample was mixed with 400 µl oxidizing solution that contained 1.4% chloramine-T, 10% N-propanol, and 80% citrate-acetate buffer in PBS. Lung samples were then incubated for 20 minutes. Samples were finally incubated for 30 minutes at 65°C shortly after adding Ehrlich's solution (Sigma-Aldrich). The reaction absorbance was measured at 550 nm. Sample concentrations were determined from the standard curve generated using trans-4-hydroxy-l-proline (Sigma-Aldrich). A standard curve was generated using trans-4-hydroxy-l-proline (Sigma-Aldrich). Hydroxyproline levels were expressed as micrograms hydroxyproline per microgram of lung tissue samples.

Public bulk and single-cell RNA-sequencing dataset acquisition

The gene expression and cell type annotation of bulk and single-cell RNA-sequencing data from lungs of normal and IPF human (GSE124685, GSE132771), of control and bleomycin-treated mice (GSE110533, GSE132771) were downloaded from the Gene Expression Omnibus.

scRNA-seq data processing

DESeq2[12], Seurat (version 2.3.2) and Scanpy (1.4.4.post1[13, 14]) were used to perform the bulk and single-cell RNA-seq data processing following the standard procedure (mentioned at https://scanpy.tutorials.readthedocs.io/en/latest/pbmc3k.html and https://satijalab.org/seurat/v3.1/pbmc3k_tutorial.html).

References

1. Weng T, Ko J, Masamha CP, Xia Z, Xiang Y, Chen NY, Molina JG, Collum S, Mertens TC, Luo F, Philip K, Davies J, Huang J, Wilson C, Thandavarayan RA, Bruckner BA, Jyothula SS, Volcik KA, Li L, Han L, Li W, Assassi S, Karmouty-Quintana H, Wagner EJ, Blackburn MR. Cleavage factor 25 deregulation contributes to pulmonary fibrosis through alternative polyadenylation. *J Clin Invest* 2019: 129(5): 1984-1999.
2. Konigshoff M, Kramer M, Balsara N, Wilhelm J, Amarie OV, Jahn A, Rose F, Fink L, Seeger W, Schaefer L, Gunther A, Eickelberg O. WNT1-inducible signaling protein-1 mediates pulmonary fibrosis in mice and is upregulated in humans with idiopathic pulmonary fibrosis. *J Clin Invest* 2009: 119(4): 772-787.
3. Konigshoff M, Wilhelm A, Jahn A, Sedding D, Amarie OV, Eul B, Seeger W, Fink L, Gunther A, Eickelberg O, Rose F. The angiotensin II receptor 2 is expressed and mediates angiotensin II signaling in lung fibrosis. *Am J Respir Cell Mol Biol* 2007: 37(6): 640-650.
4. Eickelberg O, Pansky A, Koehler E, Bihl M, Tamm M, Hildebrand P, Perruchoud AP, Kashgarian M, Roth M. Molecular mechanisms of TGF-(beta) antagonism by interferon (gamma) and cyclosporine A in lung fibroblasts. *FASEB journal : official publication of the Federation of American Societies for Experimental Biology* 2001: 15(3): 797-806.
5. Zhang Y, Wang J, Huang W, Cai J, Ba J, Wang Y, Ke Q, Huang Y, Liu X, Qiu Y, Lu Q, Sui X, Shi Y, Wang T, Shen H, Guan Y, Zhou Y, Chen Y, Wang M, Xiang AP. Nuclear Nestin deficiency drives tumor senescence via lamin A/C-dependent nuclear deformation. *Nature communications* 2018: 9(1): 3613.
6. Lehmann M, Buhl L, Alsafadi HN, Klee S, Hermann S, Mutze K, Ota C, Lindner M, Behr J, Hilgendorff A, Wagner DE, Konigshoff M. Differential effects of Nintedanib and Pirfenidone on lung alveolar epithelial cell function in ex vivo murine and human lung tissue cultures of pulmonary fibrosis. *Respiratory research* 2018: 19(1): 175.
7. Uhl FE, Vierkotten S, Wagner DE, Burgstaller G, Costa R, Koch I, Lindner M, Meiners S, Eickelberg O, Konigshoff M. Preclinical validation and imaging of Wnt-induced repair in human 3D lung tissue cultures. *The European respiratory journal* 2015: 46(4): 1150-1166.
8. Ran FA, Hsu PD, Wright J, Agarwala V, Scott DA, Zhang F. Genome engineering using the CRISPR-Cas9 system. *Nat Protoc* 2013: 8(11): 2281-2308.
9. Ran FA, Hsu PD, Lin CY, Gootenberg JS, Konermann S, Trevino AE, Scott DA, Inoue A, Matoba S, Zhang Y, Zhang F. Double nicking by RNA-guided CRISPR Cas9 for enhanced genome editing specificity. *Cell* 2013: 154(6): 1380-1389.
10. Ehlers MD. Reinsertion or degradation of AMPA receptors determined by activity-dependent endocytic sorting. *Neuron* 2000: 28(2): 511-525.

11. Liu Y, Tao YM, Woo RS, Xiong WC, Mei L. Stimulated ErbB4 internalization is necessary for neuregulin signaling in neurons. *Biochemical and biophysical research communications* 2007: 354(2): 505-510.
12. Love MI, Huber W, Anders S. Moderated estimation of fold change and dispersion for RNA-seq data with DESeq2. *Genome Biol* 2014: 15(12): 550.
13. Butler A, Hoffman P, Smibert P, Papalexi E, Satija R. Integrating single-cell transcriptomic data across different conditions, technologies, and species. *Nat Biotechnol* 2018: 36(5): 411-420.
14. Stuart T, Butler A, Hoffman P, Hafemeister C, Papalexi E, Mauck WM, 3rd, Hao Y, Stoeckius M, Smibert P, Satija R. Comprehensive Integration of Single-Cell Data. *Cell* 2019: 177(7): 1888-1902 e1821.

Supplementary Figure Legends

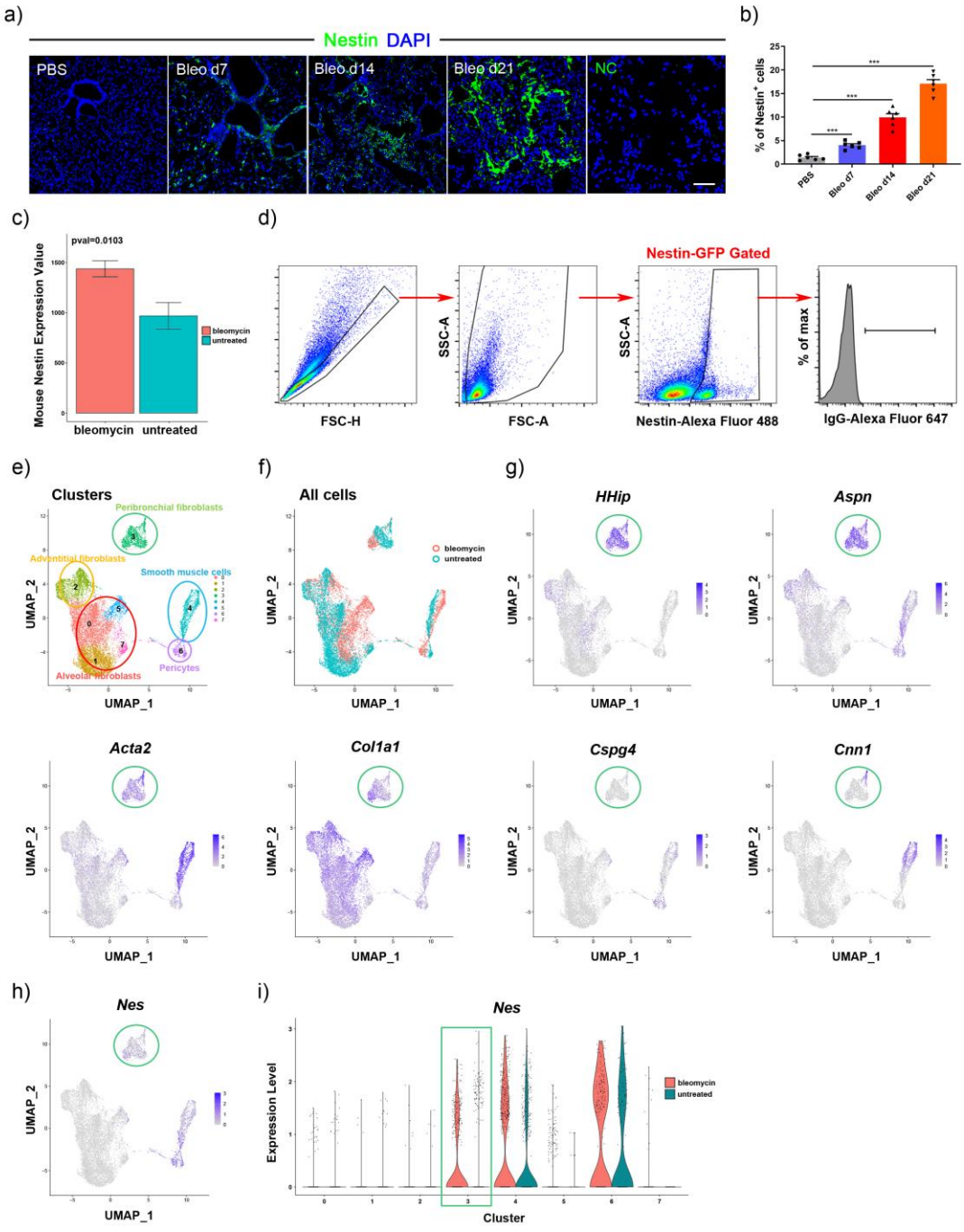

Figure S1: Nestin expression in experimental pulmonary fibrosis and RNA-seq data, and co-expression of Nestin and Collagen I, α-SMA, NG2, Calponin 1, CD31, SPC or AQP5 in mice lungs.

a) Immunofluorescence staining of Nestin in lung sections from C57/BL6 mice on day 7, 14 and 21 days after bleomycin exposure. Scale bars: 100 μm. b) Quantification of Nestin-positive cells from immunofluorescent images in a) (n=6 mice per group; five fields assessed per sample). c) Nestin gene expression extracted from GSE110533 in mice fibrotic and control lung samples. d) Gating strategies of Nestin-GFP positive cells in myofibroblasts (both α-SMA+ and Collagen I+), pericytes (NG2+), smooth muscle cells (Calponin 1+), vascular endothelial cells (CD31+), type II alveolar epithelial cells (SPC+), or type I alveolar epithelial cells (AQP5+) respectively in flow cytometry analysis. e) Cell clusters of the sc-RNA-seq data from GSE132771. f) UMAP plot of all cells of the scRNA-seq data in e). g) UMAP plots of Hhip, Aspn, Acta2, Col1a1, Cspg4 and Cnn1 of the scRNA-seq data in e). Blue indicates high expression. h) UMAP of Nestin of the scRNA-seq data in e). i) Violin plot of Nestin expression in each cell cluster. Green box indicates myofibroblast cluster. Data are presented as the mean ± SD of three independent experiments; *P<0.05, **P<0.01, ***P<0.001; One-way ANOVA and Tukey’s multiple comparisons test.

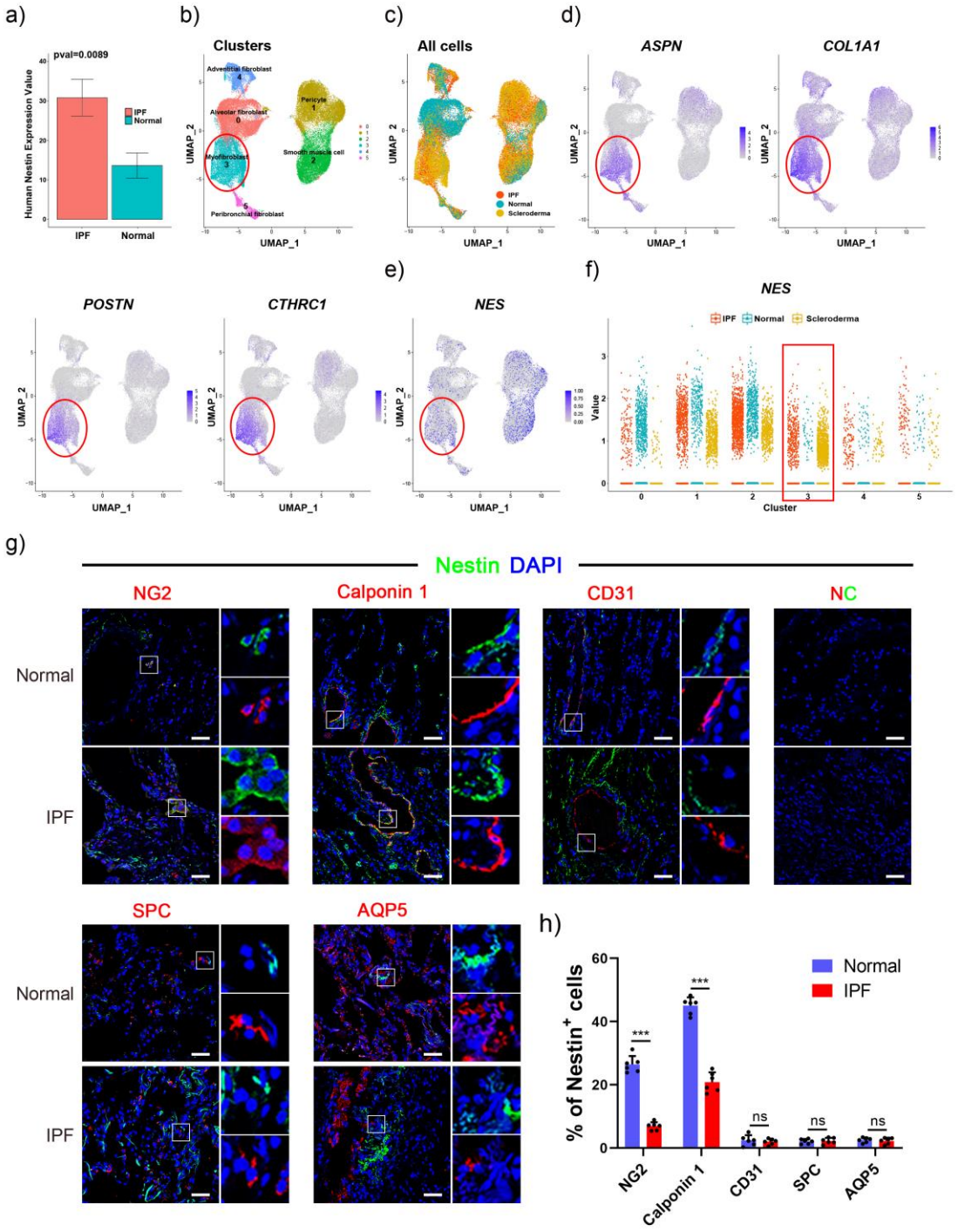

Figure S2: Nestin expression in IPF and co-localization of Nestin and Collagen I, NG2, Calponin 1, CD31, SPC or AQP5 in IPF lungs.

a) Nestin gene expression extracted from GSE124685 in IPF and control lung samples. b) Cell clusters of the sc-RNA-seq data from GSE132771. c) UMAP plot of all cells of the sc-RNA-seq data from GSE132771 in IPF and normal conditions. d) UMAP plots of ASPN, COL1A1, POSTN and CTHRC1 of the scRNA-seq data in IPF. Blue indicates high expression. e) UMAP plots of NESTIN of the scRNA-seq data in IPF. Blue indicates high expression. f) Violin plot of NESTIN in each cell cluster. Red box indicates myofibroblast cluster. g) Immunofluorescence assay was carried out to determine the co-localization of Nestin (green) and NG2 (pericytes), Calponin 1 (smooth muscle cells), CD31 (vascular endothelial cells), SPC (type II alveolar epithelial cells) or AQP5 (type I alveolar epithelial cells) (red) respectively in IPF lungs. Scale bars: 40 μm. h) Semiquantitative scoring of double-positive cells as a percentage of Nestin-positive cells, as obtained from immunofluorescent images (n=6 per group; five fields assessed per sample). Data are presented as the mean ± SD of three independent experiments; *P<0.05, **P<0.01, ***P<0.001; One-way ANOVA and Tukey's multiple comparisons test.

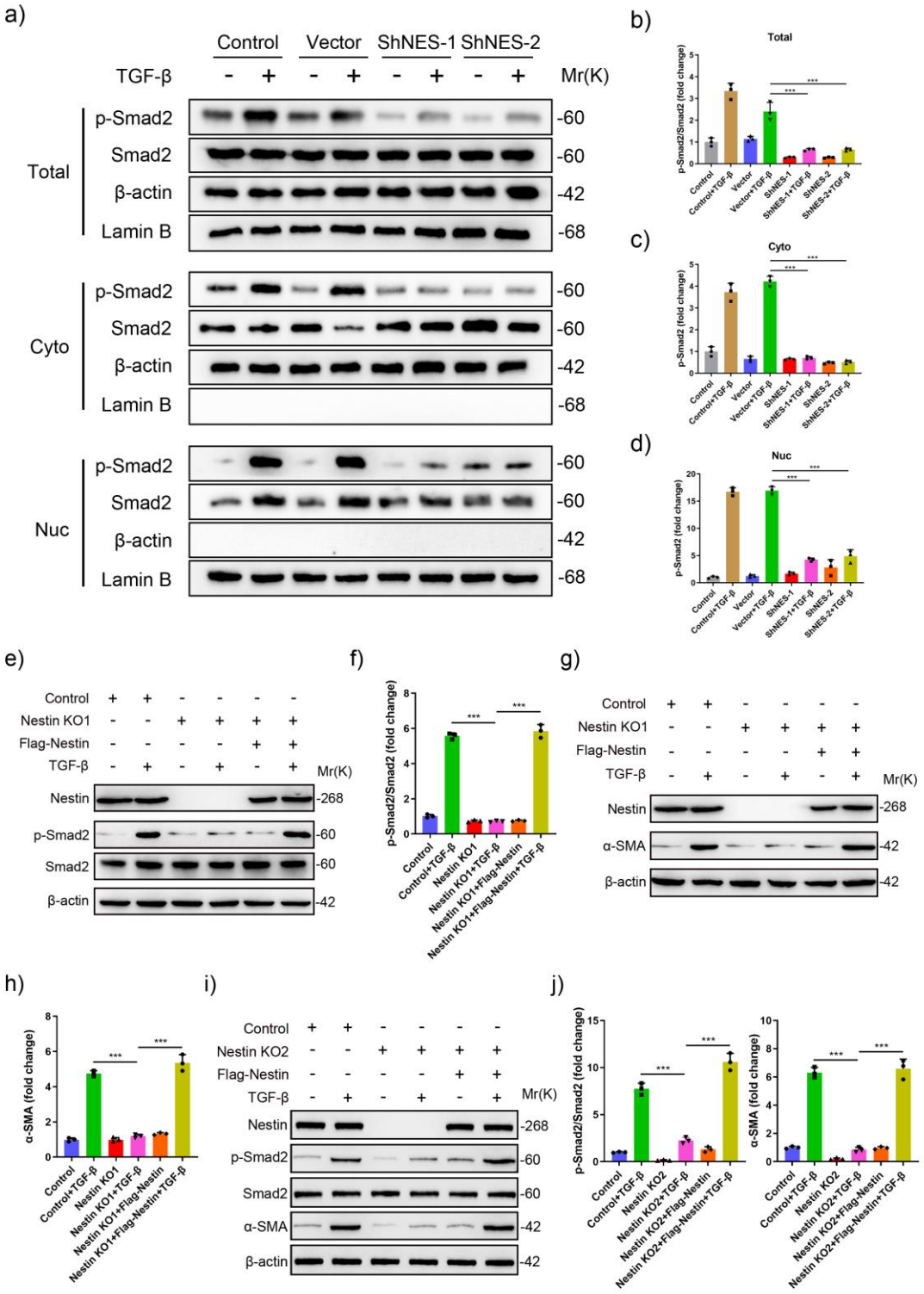
a)
Control
Vector
ShNES-1
ShNES-2
TGF-β
Mr(K)
Total
Cyto
Nuc
p-Smad2
Smad2
β-actin
Lamin B
-60
-42
-68
b)
Total
c)
Cyto
d)
Nuc
p-Smad2/Smad2 (fold change)
p-Smad2 (fold change)
Control
Control+TGF-β
Vector
Vector+TGF-β
ShNES-1
ShNES-1+TGF-β
ShNES-2
ShNES-2+TGF-β
e)
Nestin KO1
Flag-Nestin
Nestin
-268
f)
Nestin KO1+TGF-β
Nestin KO1+Flag-Nestin
Nestin KO1+Flag-Nestin+TGF-β
g)
α-SMA
-42
h)
α-SMA (fold change)
i)
Nestin KO2
j)
Nestin KO2+TGF-β
Nestin KO2+Flag-Nestin
Nestin KO2+Flag-Nestin+TGF-β

Figure S3: Nestin knockdown inhibits TGF-β/Smad signaling.

a) Immunoblotting analysis of p-Smad2 and Smad2 protein levels in nucleus and cytoplasm. Control and Nestin-knockdown primary mouse lung fibroblasts were treated with or without TGF-β (5 ng/ml). b-d) Quantification of p-Smad2 and Smad2 levels in total, cytoplasmic and nuclear cell lysates (n=3 per group). e) Western blot analysis and f) quantification of p-Smad2 and Smad2 levels with CRISPR/Cas9-mediated Nestin knockout (Nestin KO1) or overexpression of Nestin treated with or without TGF-β (5 ng/ml) in MRC5s (n=3 per group). g) Western blot analysis and h) quantification of α-SMA levels with CRISPR/Cas9-mediated Nestin knockout (Nestin KO1) or overexpression of Nestin treated with or without TGF-β (5 ng/ml) in MRC5s (n=3 per group). i) Western blot analysis and j) quantification of p-Smad2, Smad2 and α-SMA levels with CRISPR/Cas9-mediated Nestin knockout (Nestin KO2) or overexpression of Nestin treated with or without TGF-β (5 ng/ml) in MRC5s (n=3 per group). Data are presented as the mean ± SD of three independent experiments; *P<0.05, **P<0.01, ***P<0.001; One-way ANOVA and Tukey's multiple comparisons test.

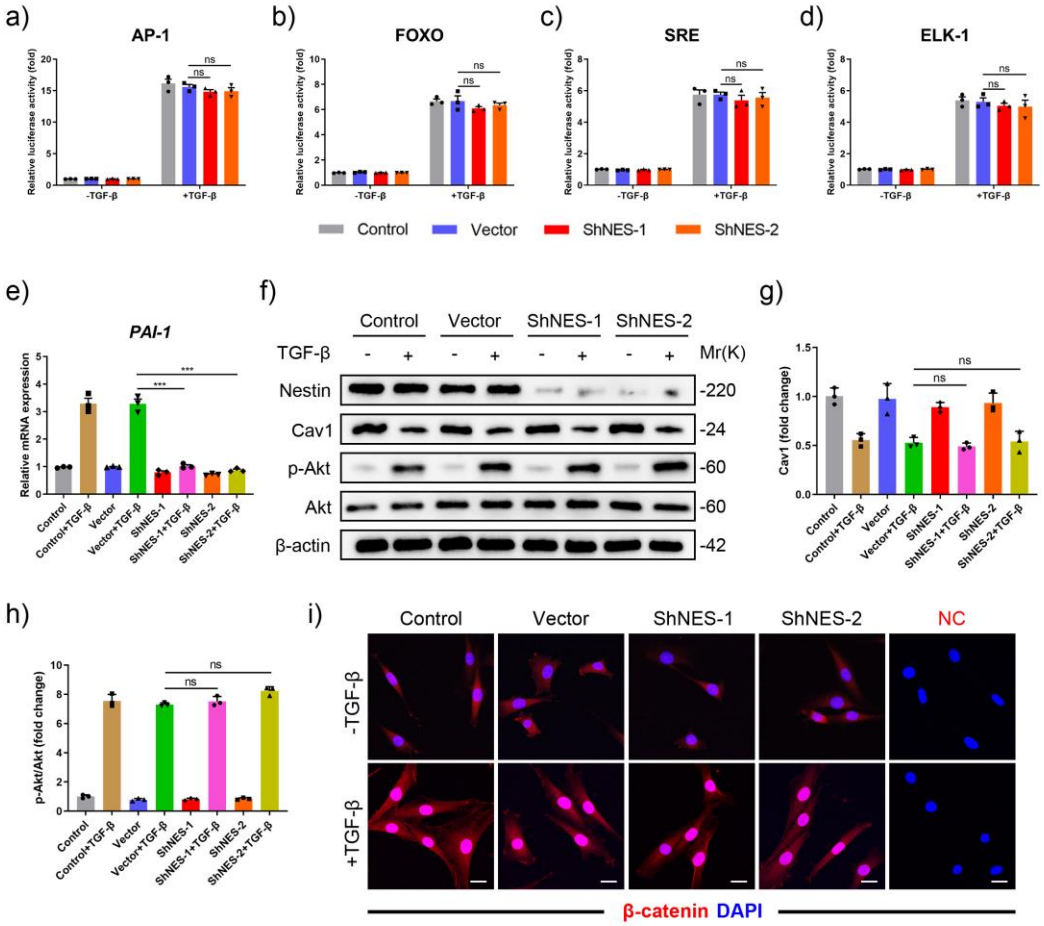

Figure S4: The effect of Nestin on the activity of non-smad TGF-β pathways.

a-d) Nestin-knockdown primary mouse lung fibroblasts were transfected with pGL3-SRE, pGL3-FOXO, pGL3-AP-1 and pGL3-ELK-1 luciferase reporters and treated with or without TGF-β (5 ng/ml) for 24 hours, and luciferase activities were measured (n=3 per group). e) qPCR analysis of PAI-1 mRNA expression in Nestin-knockdown primary mouse lung fibroblasts (n=3 per group). f) Western blot analysis and g-h) quantification of Cav1, p-Akt and Akt expression in Nestin-knockdown primary mouse lung fibroblasts treated for 72

hours with or without TGF-β (5 ng/ml) (n=3 per group). i) Immunofluorescence staining of Nestin-knockdown primary mouse lung fibroblasts treated with or without TGF-β (5 ng/ml) and visualized using anti-β-catenin (red). Scale bars: 20 μm. Data are presented as the mean ± SD of three independent experiments; *P<0.05, **P<0.01, ***P<0.001; One-way ANOVA and Tukey's multiple comparisons test.

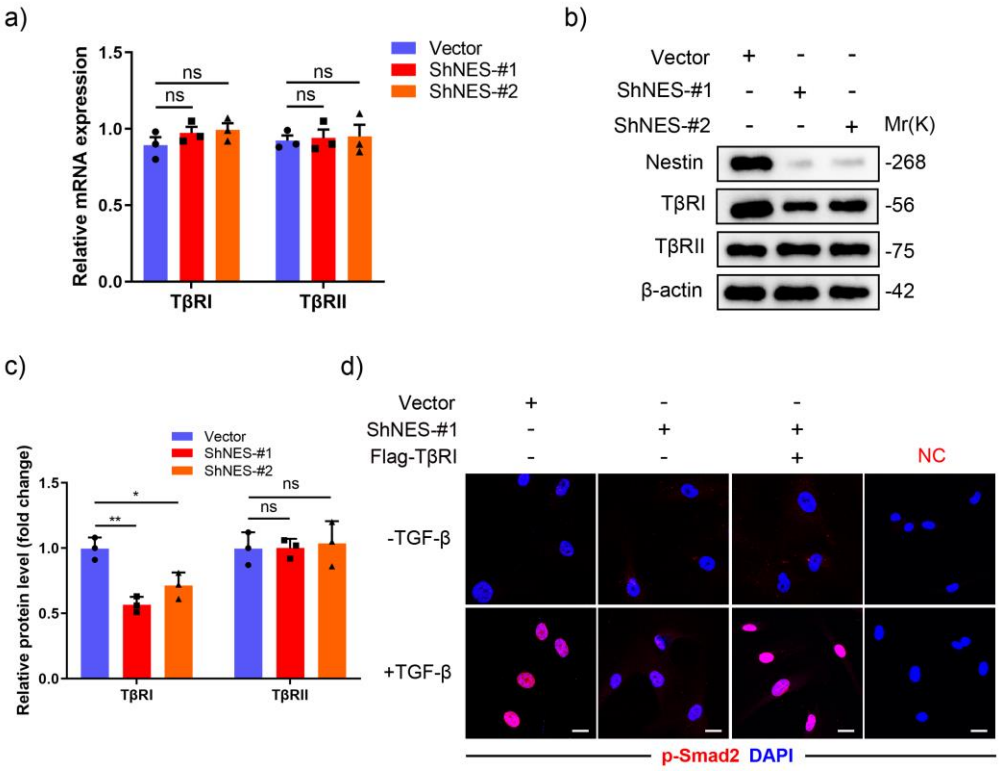

Figure S5: Nestin knockdown inhibits TGF-β/Smad signaling via regulating TβRI stability in MRC5s.

a) qPCR analysis of TβRI and TβRII mRNA expression in Nestin-knockdown MRC5s (n=3 per group). b) Western blot analysis and c) quantification of TβRI and TβRII expression in Nestin-knockdown MRC5s (n=3 per group). d) Immunofluorescence staining of p-Smad2 in MRC5s with Nestin knockdown and overexpression of TβRI treated with or without TGF-β (5 ng/ml). Scale bars: 20 μm. Data are presented as the mean ± SD of three independent experiments; **P*<0.05, ***P*<0.01, ****P*<0.001; One-way ANOVA and Tukey's multiple comparisons test.

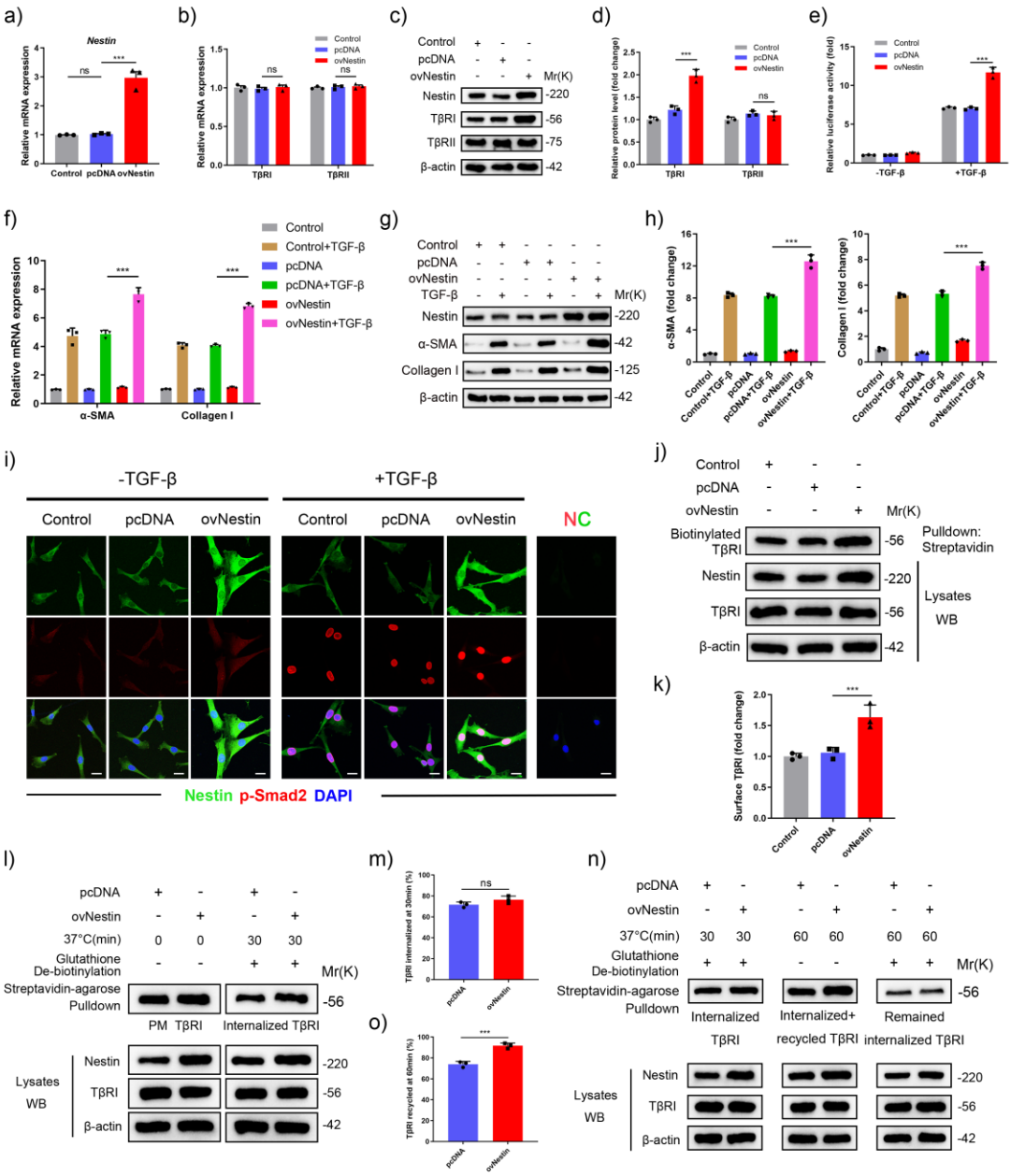

Figure S6: Nestin overexpression promotes TGF-β/Smad signaling and TβRI recycling.

a) qPCR analysis of Nestin expression in Nestin-overexpressed primary mouse lung fibroblasts (n=3 per group). b) qPCR analysis of TβRI and TβRII mRNA expression levels in Nestin-overexpressed primary mouse lung fibroblasts (n=3 per group). c) Western blot analysis and d) quantification of

TβRI and TβRII expression in Nestin-overexpressed primary mouse lung fibroblasts (n=3 per group). e) Nestin-overexpressed primary mouse lung fibroblasts were transfected with pGL3-SBE9-luciferase constructs and treated with or without TGF-β (5 ng/ml) for 24 hours, and luciferase activity was measured (n=3 per group). f) qPCR analysis of α-SMA and Collagen I expression in Nestin-overexpressed primary mouse lung fibroblasts (n=3 per group). g) Western blot analysis and h) quantification of α-SMA and Collagen I expression treated with or without TGF-β (5 ng/ml) in Nestin-overexpressed primary mouse lung fibroblasts (n=3 per group). i) Immunofluorescence staining of Nestin-overexpressed primary mouse lung fibroblasts treated with or without TGF-β (5 ng/ml) and visualized using anti-Nestin (green) and anti-p-Smad2 (red). Scale bars: 20 μm. j) Detect the protein levels of TβRI on the plasma membrane in biotinylated serum-starved Nestin-overexpressed primary mouse lung fibroblasts after treated with Chlq (100μM) for 4h. k) quantification of surface TβRI protein levels in j) (n=3 per group). l) Biotinylated serum-starved Nestin-overexpressed primary mouse lung fibroblasts were placed at 37°C for 30min and then treated with glutathione after treated with Chlq (100μM) for 4h, and then harvested and subjected to streptavidin agarose pull down and western blot analysis of TβRI, PM: plasma membrane. m) Quantification of the percentage of internalized TβRI in l) (n=3 per group); TβRI internalization rate = total internalized TβRI at 30 min / Plasma membrane TβRI × 100%. n) Western blot analysis of recycled TβRI at 60 min.

o) Quantification of the percentage of recycled TβRI in n) (n=3 per group); TβRI recycling rate = (internalized and recycled TβRI at 60 min – internalized TβRI at 60 min) / total internalized TβRI at 30 min × 100%). Data are presented as the mean ± SD of three independent experiments; *P<0.05, **P<0.01, ***P<0.001; Unpaired t test and one-way ANOVA and Tukey's multiple comparisons test.

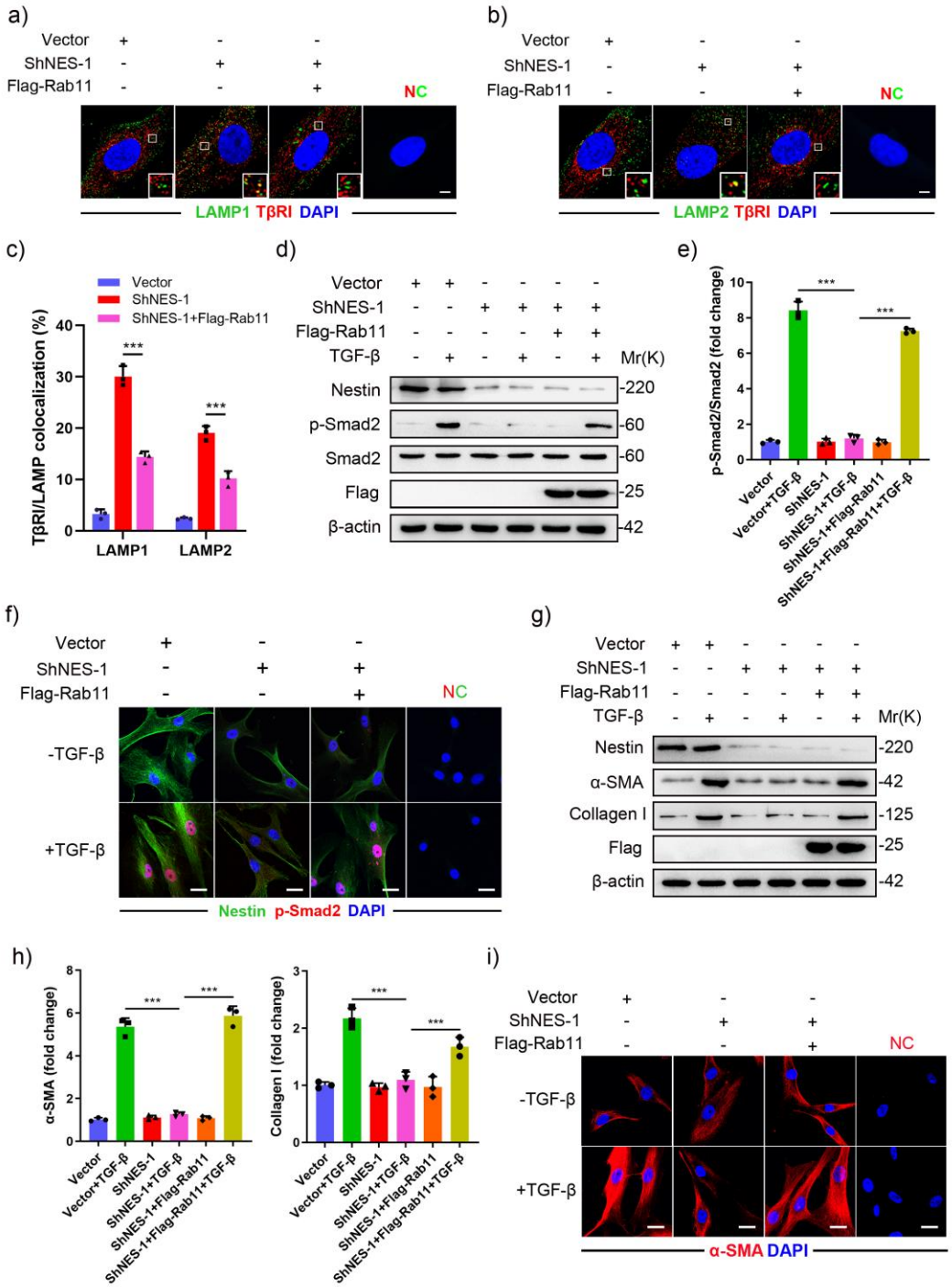

Figure S7: Rab11 is required for the ability of Nestin to promote the recycling of TβRI to the cell surface.

a) Immunofluorescence staining of TβRI and LAMP1 in Nestin-knockdown primary mouse lung fibroblasts with or without overexpression of Rab11. Scale bars: 5 μm. b) Immunofluorescence staining of TβRI and LAMP2 in Nestin-knockdown primary mouse lung fibroblasts with or without overexpression of Rab11. Scale bars: 5 μm. c) Quantification of the percentage of TβRI co-localized with LAMP1 and LAMP2. (n=3; five fields assessed per sample). d) Western blot analysis and e) quantification of p-Smad2 and Smad2 expression levels in Nestin-knockdown primary mouse lung fibroblasts with Rab11 overexpression and treated with or without TGF-β (5 ng/ml) (n=3 per group). f) Immunofluorescence staining of p-Smad2 and Nestin in Nestin-knockdown primary mouse lung fibroblasts with Rab11 overexpression and treated with or without TGF-β (5 ng/ml). Scale bars: 20 μm. g) Western blot analysis and h) quantification of α-SMA and Collagen I expression levels in Nestin-knockdown primary mouse lung fibroblasts with Rab11 overexpression and treated with or without TGF-β (5 ng/ml) (n=3 per group). i) Immunofluorescence staining of α-SMA in Nestin-knockdown primary mouse lung fibroblasts with Rab11 overexpression and treated with or without TGF-β (5 ng/ml). Scale bars: 20 μm. Data are presented as the mean ± SD of three independent experiments; *P<0.05, **P<0.01, ***P<0.001; One-way ANOVA and Tukey's multiple comparisons test.

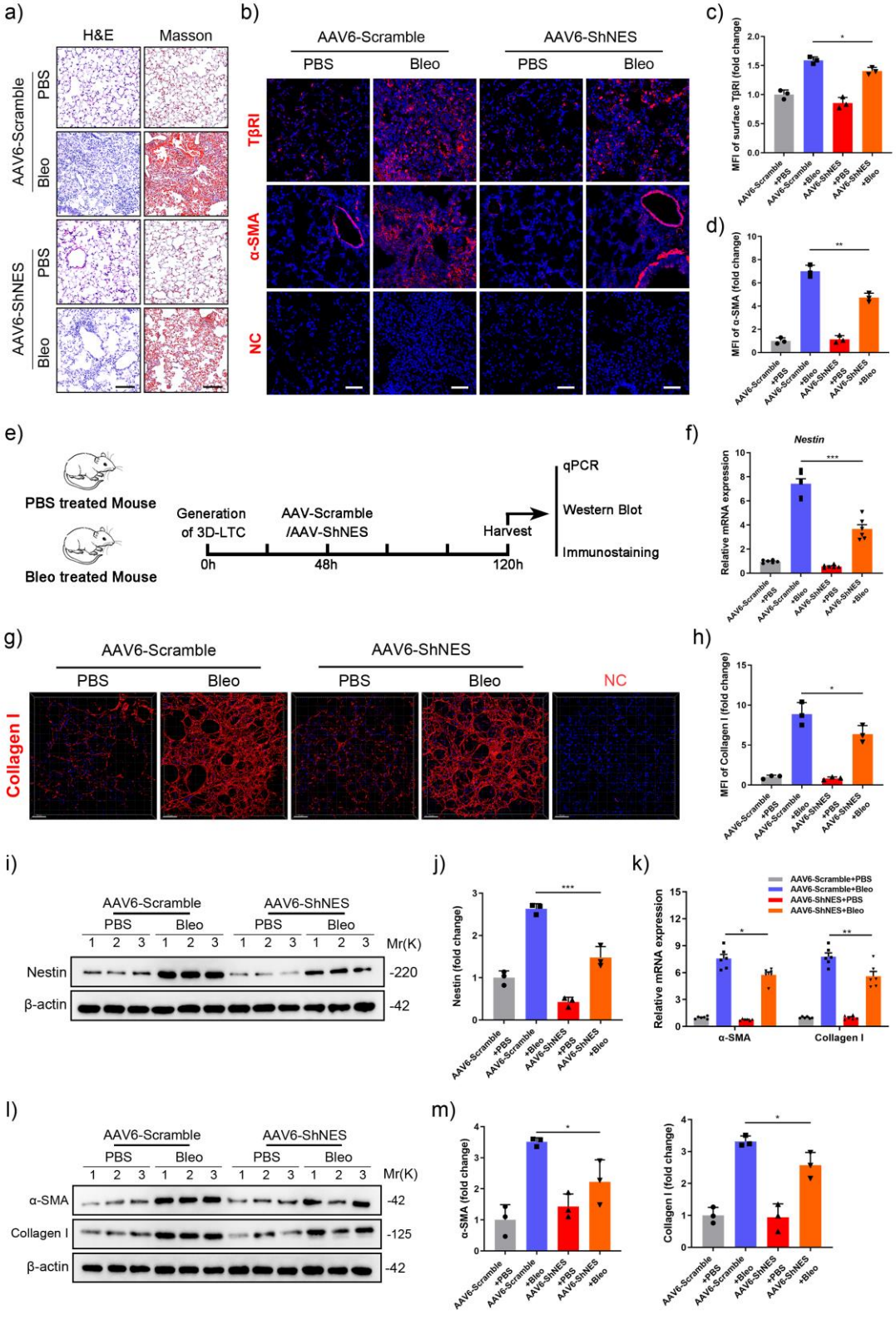

Figure S8: Downregulation of Nestin attenuates pulmonary fibrosis in bleomycin-induced pulmonary fibrosis model and 3D-LTC.

a) H&E staining and Masson's trichrome staining in lung sections from C57/BL6 mice of the different groups. Scale bars: 100 μm. b) Immunofluorescence staining with surface TβRI and α-SMA in lung sections from C57/BL6 mice of the different groups. Scale bars: 50 μm. c-d) Mean fluorescence intensity of surface TβRI and α-SMA in lung sections from C57/BL6 mice of the different groups (n=3; five fields assessed per sample). e) Experimental design. 8-week-old C57BL/6 mice were intratracheally injected with bleomycin (3U/kg) or PBS. Three weeks after the bleomycin, 3D-LTC was performed and treated with AAV6-ShNES or AAV6-Scramble after 48h. Samples were collected for analysis 72h after AAV6 administration. f) qPCR analysis of Nestin mRNA expression in lung slices from the different groups (n=6 mice per group). g) Immunofluorescence staining with collagen I in lung slices from the different groups. Scale bars: 70 μm. h) Mean fluorescence intensity of collagen I in lung slices from the different groups (n=3; five fields assessed per sample). i) Western blot analysis and j) quantification of Nestin expression levels in 3D-LTCs of the different groups (n=3 per group). k) qPCR analysis of α-SMA and Collagen I mRNA expression levels in 3D-LTCs of the different groups (n=6 mice per group). l) Western blot analysis and m) quantification of α-SMA, Collagen I expression levels in 3D-LTCs of the different groups (n=3 per group). Data are presented as the mean ± SD of three independent experiments; **P*<0.05, ***P*<0.01, ****P*<0.001; Unpaired *t* test and one-way ANOVA and Tukey's multiple comparisons test.

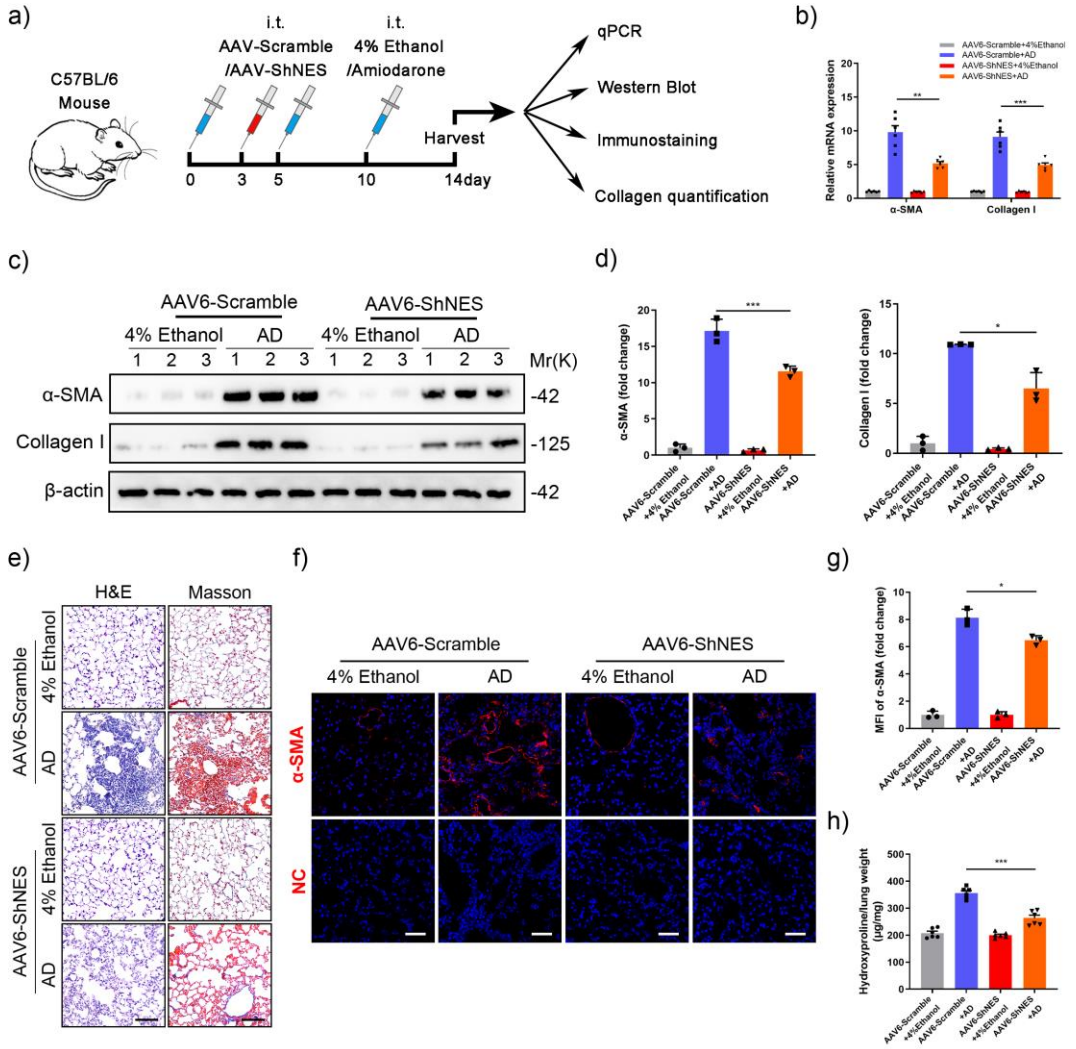

Figure S9: Downregulation of Nestin attenuates pulmonary fibrosis in amiodarone-induced mouse pulmonary fibrosis model.

a) Experimental design. 8-week-old C57BL/6 mice were intratracheally injected with amiodarone (0.8mg/kg/d) or 4% Ethanol. The mice were intratracheally injected with AAV6-ShNES or AAV6-Scramble three days after first amiodarone administration. Samples were collected for analysis 14 days after first amiodarone administration. b) qPCR analysis of α-SMA and Collagen I mRNA expression levels in lungs from C57/BL6 mice of the different groups

(n=6 mice per group). c) Western blot analysis and d) quantification of α-SMA, Collagen I expression levels in lungs from C57/BL6 mice of the different groups (n=3 per group). e) H&E staining and Masson's trichrome staining in lung sections from C57/BL6 mice of the different groups. Scale bars: 100 μm. f) Immunofluorescence staining of α-SMA in lung sections from C57/BL6 mice of the different groups. Scale bars: 50 μm. g) Mean fluorescence intensity of α-SMA in lung sections from C57/BL6 mice of the different groups (n=3; five fields assessed per sample). h) Hydroxyproline levels in lungs of C57/BL6 mice from the different groups (n=6 mice per group). Data are presented as the mean ± SD of three independent experiments; *P<0.05, **P<0.01, ***P<0.001; One-way ANOVA and Tukey's multiple comparisons test.

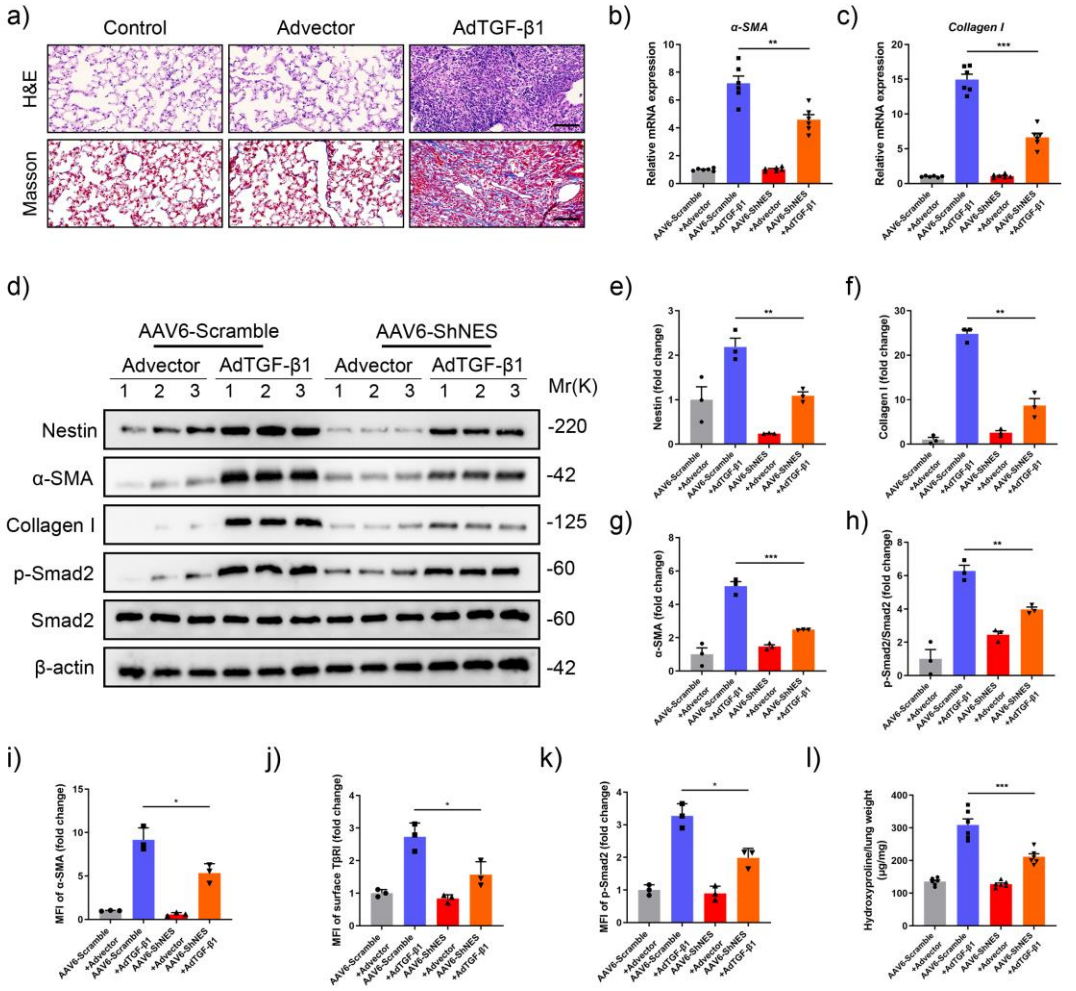

Figure S10: Downregulation of Nestin attenuates pulmonary fibrosis in TGF-β overexpression-induced pulmonary fibrosis model.

a) H&E staining and Masson's trichrome staining in lung sections from C57/BL6 mice of the different groups. Scale bars: 100 μm. qPCR analysis of b) α-SMA and c) Collagen I mRNA expression levels in lungs from C57/BL6 mice of the different groups (n=6 mice per group). d) Western blot analysis and quantification of e) Nestin, f) Collagen I, g) α-SMA, h) p-Smad2 and Smad2 expression levels in lungs from C57/BL6 mice of the different groups (n=3 per group). Mean fluorescence intensity of i) collagen I, j) TβRI and k) p-Smad2 in

lung slices from the different groups as obtained from images in figure 7k (n=3; five fields assessed per sample). l) Hydroxyproline levels in lungs of C57/BL6 mice from the different groups (n=6 mice per group). Data are presented as the mean ± SD of three independent experiments; *P<0.05, **P<0.01, ***P<0.001; One-way ANOVA and Tukey's multiple comparisons test.

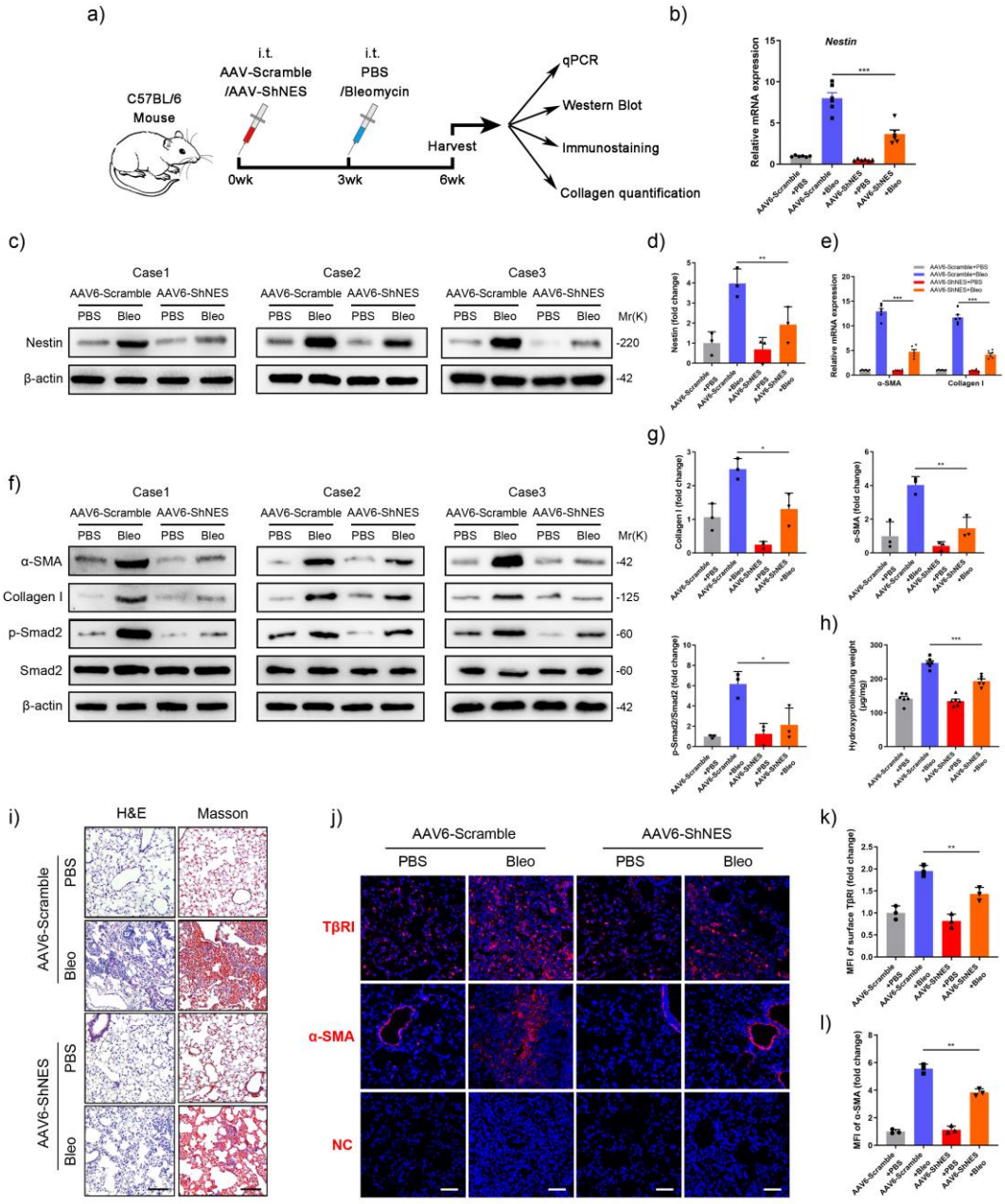

Figure S11: Downregulation of Nestin exerts preventive effects on bleomycin-induced pulmonary fibrosis in mice.

a) Experimental design. 8-week-old C57BL/6 mice were intratracheally injected with AAV6-ShNES or AAV6-Scramble. 21 days after the AAV administration, the mice were intratracheally injected with bleomycin (3U/kg) or

PBS. Samples were collected for analysis 21 days after bleomycin administration. b) qPCR analysis of Nestin mRNA expression in the lungs of C57/BL6 mice from the different groups (n=6 mice per group). c) Western blot analysis and d) quantification of Nestin expression levels in lungs from C57/BL6 mice of the different groups (n=3 per group). e) qPCR analysis of α-SMA and Collagen I mRNA expression levels in lungs from C57/BL6 mice of the different groups (n=6 mice per group). f) Western blot analysis and g) quantification of α-SMA, Collagen I, p-Smad2 and Smad2 expression levels in lungs from C57/BL6 mice of the different groups (n=3 per group). h) Hydroxyproline levels in lungs of C57/BL6 mice from the different groups (n=6 mice per group). i) H&E staining and Masson's trichrome staining in lung sections from C57/BL6 mice of the different groups. Scale bars: 100 μm. j) Immunofluorescence staining with surface TβRI and α-SMA lung sections from C57/BL6 mice of the different groups. Scale bars: 50 μm. k-l) Mean fluorescence intensity of surface TβRI and α-SMA in lung sections from C57/BL6 mice of the different groups (n=3; five fields assessed per sample). Data are presented as the mean ± SD of three independent experiments; **P*<0.05, ***P*<0.01, ****P*<0.001; One-way ANOVA and Tukey's multiple comparisons test.

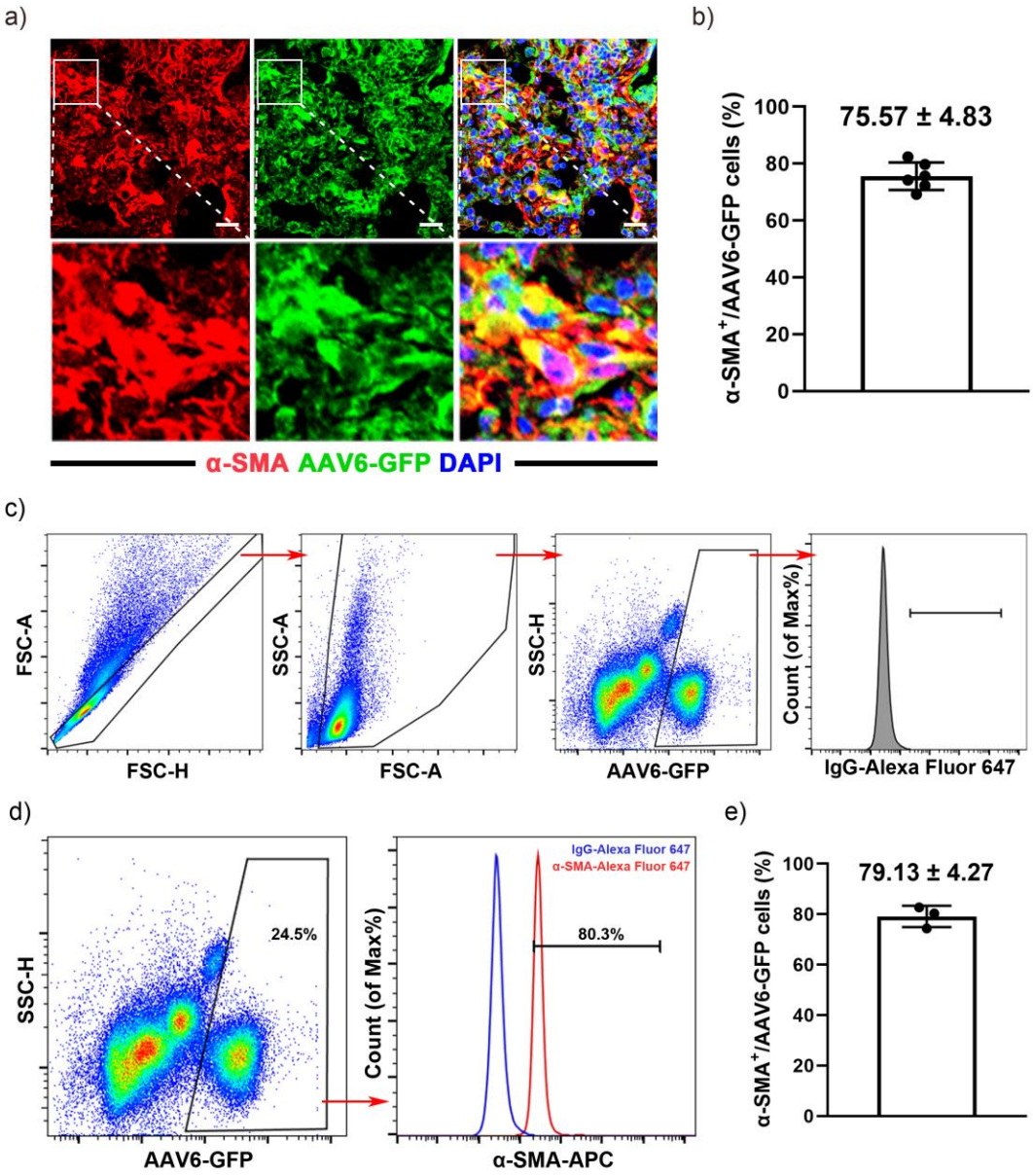

Figure S12: AAV6 exposure targets α-SMA positive myofibroblasts in bleomycin-induced mouse pulmonary fibrosis model.

a) Immunofluorescence was carried out to determine the co-localization of AAV6-GFP (green) and α-SMA (red). Scale bars: 20 μm. b) Statistical analysis of efficacy of AAV6 transduction in α-SMA positive myofibroblasts (n=6 mice per group; five fields assessed per sample). c) Gating strategies of AAV6-GFP

positive cells in myofibroblasts (α-SMA+). d) Flow cytometry was carried out to determine cell specificity of the AAV exposure. e) Statistical analysis of efficacy of AAV6 transduction in α-SMA positive myofibroblasts (n=3 mice per group). Data are presented as the mean ± SD.

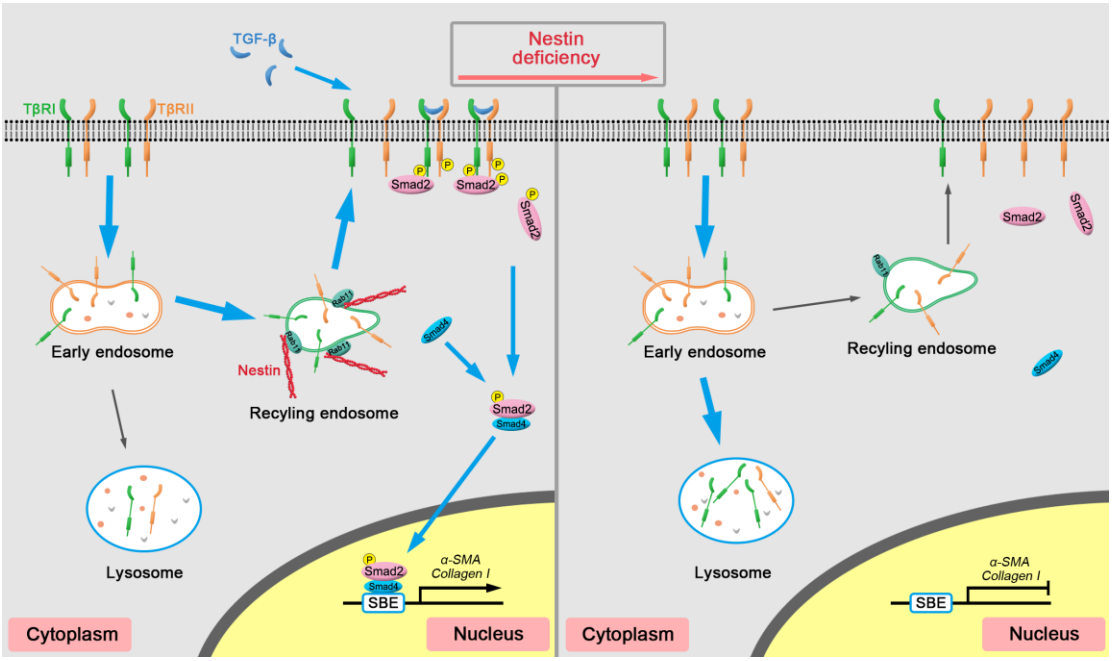

Figure S13: Illustration of Nestin-TβRI-Rab11 trimeric complexes in the regulation of pulmonary fibrosis.

Some endosomal TGF-β receptors are recycled to the plasma membrane while others are sorted to late endosomes/lysosomes for degradation. Nestin can form trimeric complexes with TβRI and Rab11. Nestin knockdown inhibits the recycling of TβRI to the cell surface in a Rab11-dependent manner and promotes the degradation of TβRI via lysosome-dependent way, thereby suppressing TGF-β/Smad signaling.

Fig 1e

Fig 2d

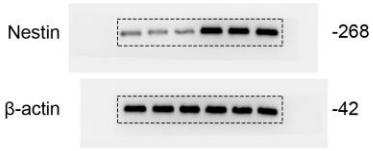

Fig 3e

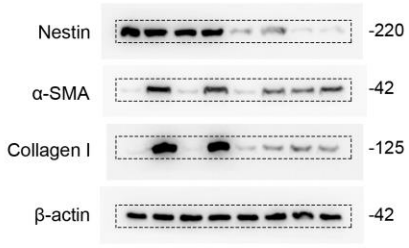

Fig 3g

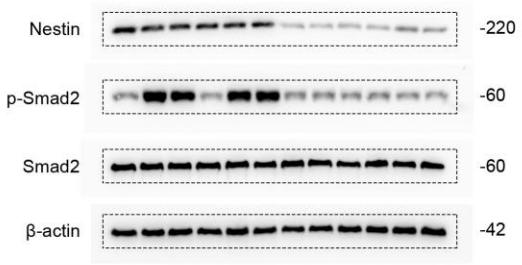

Fig 4b

Fig 4d

Fig 4f

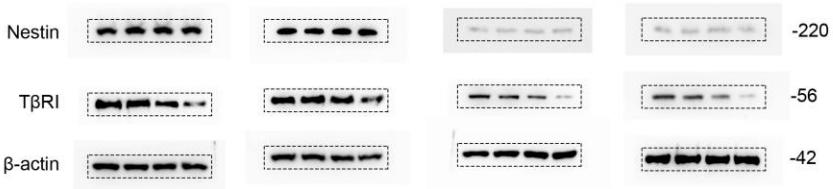

Fig 4h

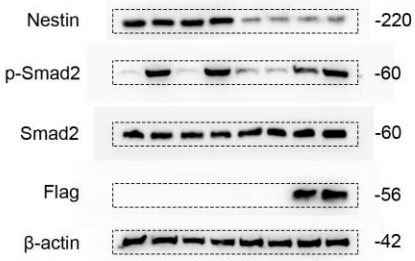

Fig 4k

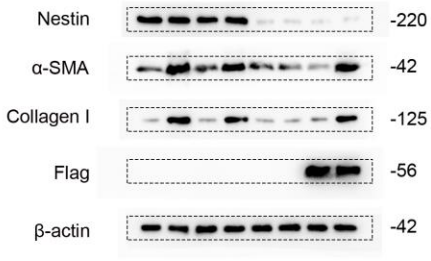

Fig 5b

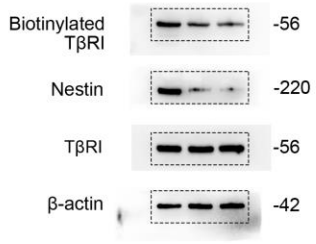

Fig 5f

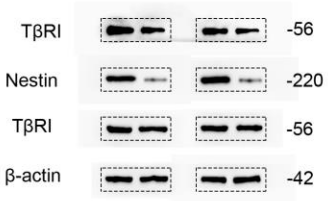

Fig 5h

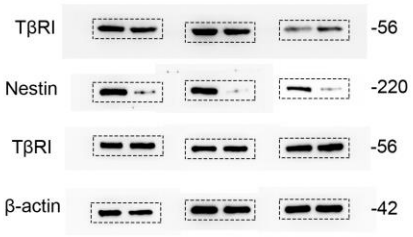

Fig 5l

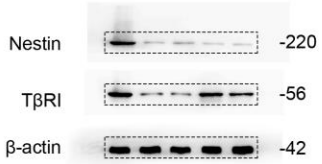

Fig 6a

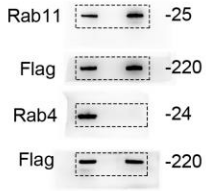

Fig 6d

Fig 6h

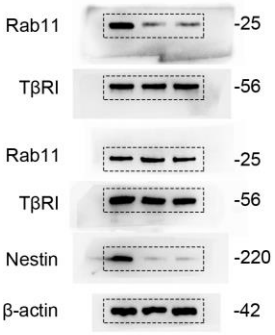

Fig 6i

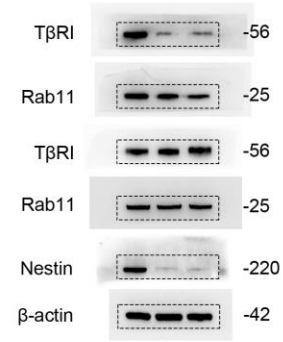

Fig 7c

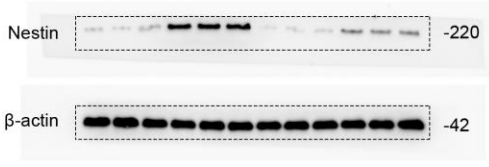

Fig 7f

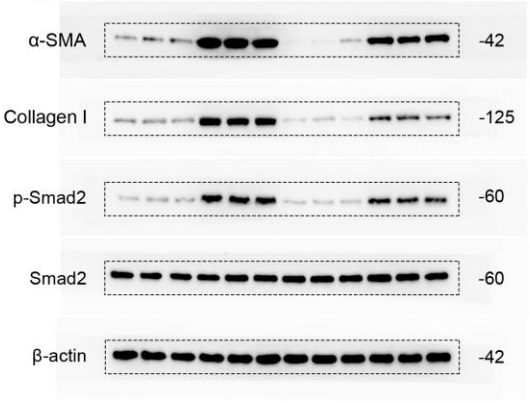

Fig 8d

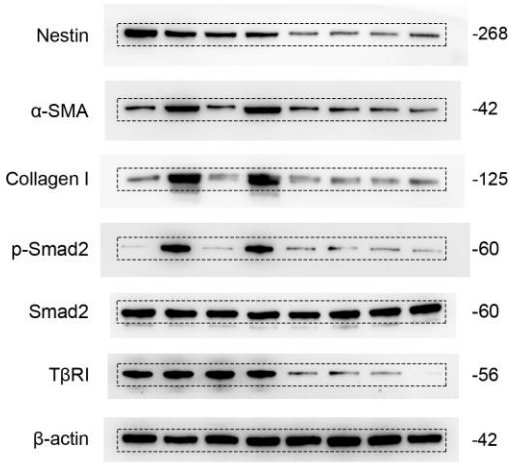

sFig 3a

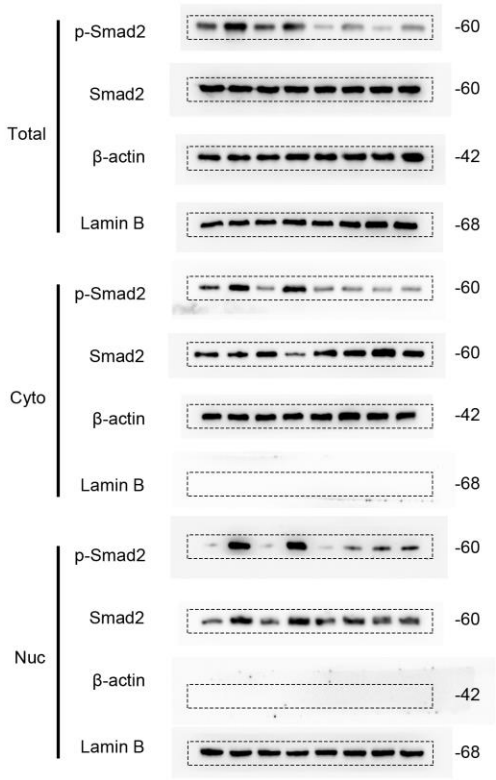

sFig 3e

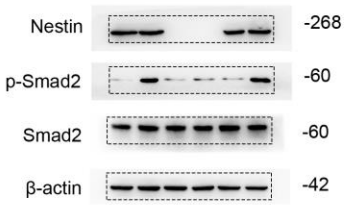

sFig 3g

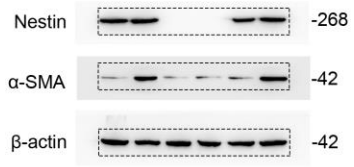

sFig 4f

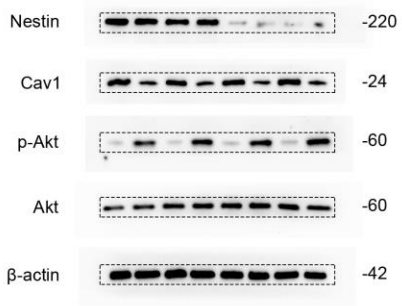

sFig 3i

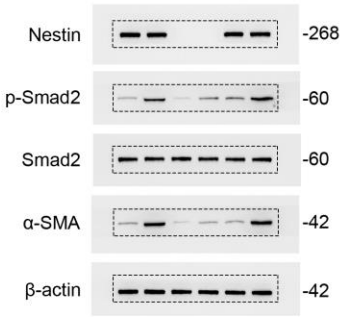

sFig 5b

sFig 6c

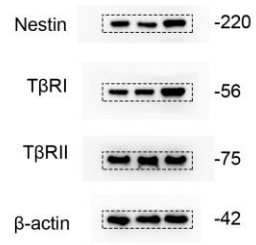

sFig 6g

sFig 6j

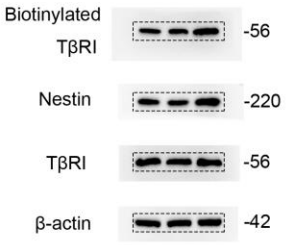

sFig 6l

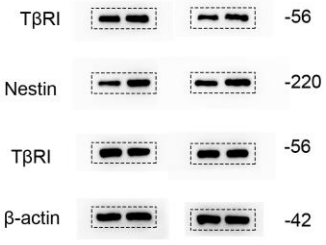

sFig 6n

sFig 7d

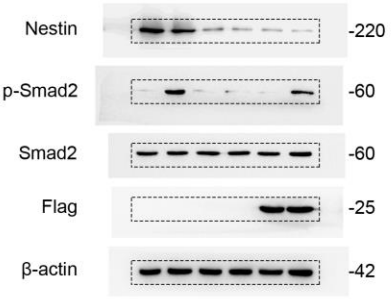

sFig 7g

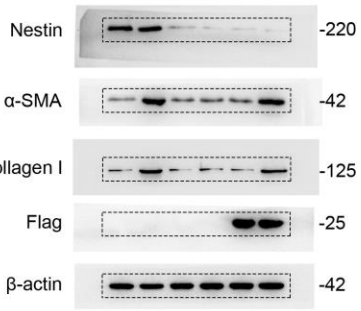

sFig 8i

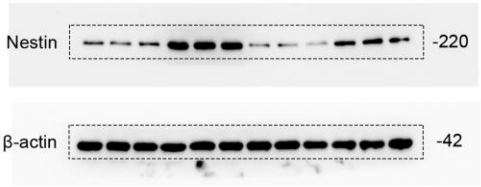

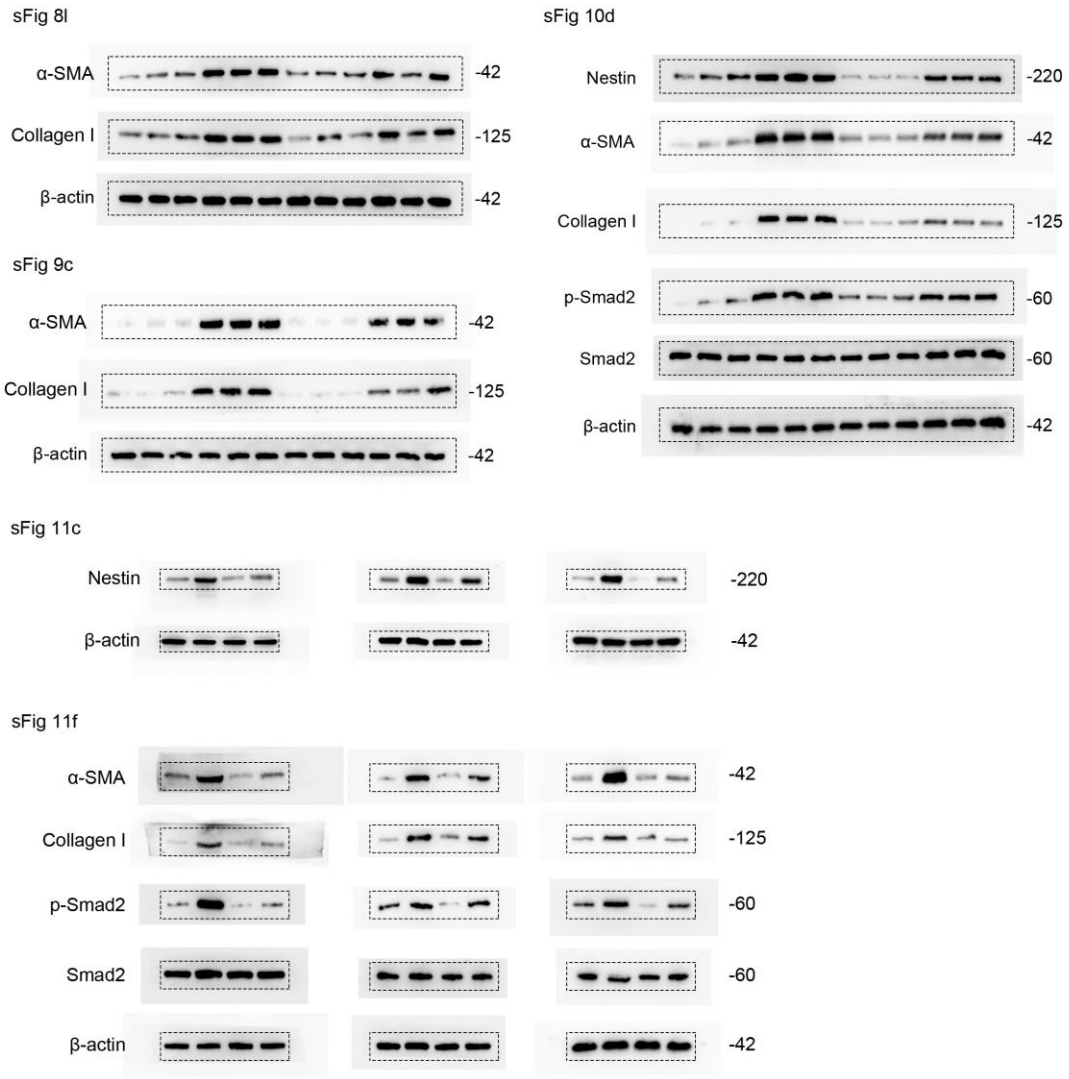

Figure S14-S18. Full length images of immunoblots.

Table S1. Clinicopathological variables and quantification for Nestin expression by staining scores in freshly IPF clinical samples.

Patient No.	Gender	Age(y)	Smoking status	FVC% pred	FVC absolute L	FEV1% pred	FEV_1 absolute L	DLCO% pred	TLC% pred	Nestin staining score
#1	M	62	Y	73.8	2.45	69.725	1.84	22.6	54.77	3
#2	M	73	N	54.22	1.72	64.71	1.57	42.5	46.4	6
#3	F	31	Y	45.87	1.43	45.65	1.24	33.6	62.9	9
#4	M	60	Y	62.33	2.32	70	2.05	76	61	4
#5	M	51	N	48.33	2.32	50	1.74	36.4	44.3	12
#6	M	68	N	65.63	1.81	79.77	1.72	49.7	59.4	1
#7	M	68	Y	49	1.71	53	1.44	29	42	8
#8	M	69	Y	90.33	2.42	98	2.06	66	74	2
#9	M	59	N	81.33	2.6	93	2.4	79	70	2
#10	M	62	N	84	3.08	91.3	2.63	82	75	1
#11	M	62	Y	83.33	3.09	91.48	2.52	60.84	72.36	2
#12	M	52	Y	54.94	2.11	61.95	1.93	29.8	52.5	16
#13	M	65	N	70.83	2.62	72.74	2.1	44.5	58.8	4
#14	M	54	N	80	3.64	85.6	3.09	73	77	6
#15	M	51	Y	62.29	2.28	65.54	1.96	41.8	58.6	16
#16	M	65	N	82.36	3.12	86.85	2.57	71	74.3	2
#17	M	57	Y	90.62	3.65	93.1	2.99	47.2	73.8	1
#18	F	48	N	77.37	2.09	78.99	1.82	49.78	74.28	4
#19	M	56	Y	100.89	3.8	106.55	3.22	47.18	73.37	1
#20	M	66	Y	58.28	1.98	66.3	1.76	38.74	53.86	2
#21	F	66	N	92.2	2.37	94.43	2.03	52.72	69.42	4
#22	M	62	Y	68.6	2.83	74	2.39	50.2	64.2	2
#23	M	49	Y	72.03	3.11	74.28	2.6	36.89	56.48	6
#24	M	53	Y	47.18	1.73	53.95	1.61	53.5	68.1	12
#25	M	70	N	49.27	1.66	51.16	1.32	27.12	43.62	12
#26	M	60	Y	104.63	4.25	87.06	2.79	42.3	76.6	4
#27	F	49	N	44.42	1.22	49.35	1.15	48.4	25.6	12
#28	M	59	Y	48.65	1.84	54.11	1.62	14.98	45.05	12
#29	M	67	Y	74.22	2.12	86.29	1.98	47.53	57.06	2
#30	M	63	Y	68.33	2.74	71.95	2.26	47.16	62.99	3
#31	M	61	Y	38.1	1.47	45.78	1.4	19.2	24.6	12
#32	M	70	Y	55	1.85	66	1.71	36	54	3
#33	F	28	N	67.5	2.33	72.3	2.17	51.15	75.13	1
#34	M	66	Y	104.34	3.78	111.66	3.15	84.9	86.4	1
#35	F	61	N	66.23	1.6	69.17	1.4	55.4	62.3	4

IPF: idiopathic pulmonary fibrosis; % pred: % predicted; FVC: forced vital capacity; FEV1: forced expiratory volume in 1 s; DLCO: diffusing capacity of the lung for carbon monoxide; TLC: total lung capacity.

Table S2. Summary of clinicopathological characteristics of study subjects.

Variable	IPF	Controls
Subjects	35	13
Male %	82.86	53.85
Age years	58.94±9.94	49.91±8.30
Ever-smoker %	60.00	15.38
FVC% pred	69.04±18.03	100.62±12.79
FVC absolute L	2.43±0.77	3.43±1.03
FEV_1% pred	73.88±17.59	94.79±12.03
FEV_1 absolute L	2.06±0.57	2.76±0.82
DLCO% pred	48.23±17.60	
TLC% pred	60.86±14.44	

Data are presented as mean ± SD. IPF: idiopathic pulmonary fibrosis; % pred: % predicted; FVC: forced vital capacity; FEV_1: forced expiratory volume in 1 s; DLCO: diffusing capacity of the lung for carbon monoxide; TLC: total lung capacity.

Table S3: Target sequences of shRNAs. Related to Experimental Procedures.

Name	Sequences (5′ to 3′)
Human：	
NESTIN shRNA#1	**5′-GCTAGTCCCTGCCTGAATA-3′**
NESTIN shRNA#2	**5′-GCAGACATCATTGGTGTTAAT-3′**
Mouse：	
NESTIN shRNA1	**5′-GGAAGAAGTTCCCAGGCTTCT-3′**
NESTIN shRNA2	**5′-GCTGAAGCTGCATTTCCTTGG-3′**
NESTIN shRNA（AAV-6）	**5′-GTGAGACTCTGGAATGCAA-3′**
Scramble shRNA（AAV-6）	**5′-TTCTCCGAACGTGTCACGTAA-3′**

Table S4: Primer used to amplify the human transcripts or genome DNA during PCR. Related to Experimental Procedures.

Gene	Sequences (5′ to 3′)	application
hNESTIN	**Forward: 5'-CTGCTACCCTTGAGACACCTG-3'**	**qPCR**
	Reverse: 5'-GGGCTCTGATCTCTGCATCTAC-3'	
hGAPDH	**Forward: 5'-GTCGGAGTCAACGGATTT-3'**	**qPCR**
	Reverse:5'-GGAATCATATTGGAACATGTAAACC-3'	
mNESTIN	**Forward: 5'-GCAGGAGAAGCAGGGTCTAC-3'**	**qPCR**
	Reverse: 5'-GGGGTCAGGAAAGCCAA-3'	
mActa2	**Forward: 5'-TGAGACCTTCAATGTCCCCGC-3'**	**qPCR**
	Reverse: 5'-TCACACCATCTCCAGAGTCCAGC-3'	
mCollagen I	**Forward: 5'-CCCAGAGTGGAACAGCGATT-3'**	**qPCR**
	Reverse: 5'-ATGAGTTCTTCGCTGGGGTG -3'	
mTβRI	**Forward: 5'-TGGGACTTGCTGTGAGACAT-3'**	**qPCR**
	Reverse: 5'-ATGTCAGCGCGTTTGAAGGA-3'	
mTβRII	**Forward: 5′-AACGACTTGACCTGTTGCCT-3′**	**qPCR**
	Reverse: 5′-TCCGTCTGCTTGAACGACTC-3′	
m18S	**Forward: 5'-GTGACGTTGACATCCGTAAAGA-3'**	**qPCR**
	Reverse: 5'-GCCGGACTCATCGTACTCC-3'	

Table S5: Primary and secondary antibodies.

Product	Catalogue Number	Supplier
Primary antibody:		
WB:		
mouse anti-Nestin	**611658**	**BD Biosciences**
mouse anti-Nestin	**MAB353**	**Millipore**
rabbit anti-DYKDDDDK（Flag Tag）	**14793**	**Cell Signaling Technology**
mouse anti-DYKDDDDK（Flag Tag）	**8146**	**Cell Signaling Technology**
mouse Anti-β-actin	**600081**	**Proteintech**
rabbit anti-Collagen I	**ab34710**	**Abcam**
rabbit anti-TβRI	**ab31013**	**Abcam**
rabbit anti-TβRII	**ab186838**	**Abcam**
rabbit Anti-p-Smad2	**18338**	**Cell Signaling Technology**
rabbit Anti-Smad2	**5339**	**Cell Signaling Technology**
mouse anti-α-SMA	**ab7817**	**Abcam**
rabbit anti-Rab4	**ab109009**	**Abcam**
rabbit anti-Rab11	**5589**	**Cell Signaling Technology**
mouse anti-Rab11	**610656**	**BD Biosciences**
rabbit anti-Lamin B	**12586**	**Cell Signaling Technology**
rabbit anti-Caveolin-1	**ab2910**	**Abcam**
rabbit anti-Phospho-Akt	**4060**	**Cell Signaling Technology**
rabbit anti-Akt	**4691**	**Cell Signaling Technology**

IP:

mouse anti-DYKDDDDK（Flag Tag）	**8146**	**Cell Signaling Technology**
rabbit anti-TβRI	**ab31013**	**Abcam**
rabbit anti-Rab11	**5589**	**Cell Signaling Technology**

IF:

rabbit anti-Nestin	**ABD69**	**Millipore**
mouse anti-Nestin	**MAB5326**	**Millipore**
mouse anti-Nestin	**MAB353**	**Millipore**
rabbit anti-CD31	**ab28364**	**Abcam**
rabbit anti-CD31	**ab76533**	**Abcam**
mouse anti-α-SMA	**ab7817**	**Abcam**
rabbit anti-NG2	**AB5320**	**Millipore**
rabbit anti-NG2	**ab183929**	**Abcam**
rabbit anti-Prosurfactant Protein C	**AB3786**	**Millipore**
rabbit anti-Rab11	**5589**	**Cell Signaling Technology**
mouse-anti-Rab11	**05-853**	**Millipore**
mouse anti-Aquaporin 5	**sc-514022**	**Santa Cruz Biotechnology**
rabbit anti-Aquaporin 5	**ab92320**	**Abcam**
mouse anti-TβRI	**sc-518086**	**santa crauz**
rabbit anti-Rab4	**ab109009**	**Abcam**
rabbit anti-Calponin 1	**ab46794**	**Abcam**
rabbit Anti-p-Smad2	**18338**	**Cell Signaling Technology**

rat Anti-LAMP1	**MABC39**	**Millipore**
rat Anti-LAMP2	**428019**	**Millipore**
rabbit anti-β-catenin	**ab16051**	**Abcam**
IHC:		
rabbit anti-Nestin	**ABD69**	**Millipore**
mouse anti-Nestin	**MAB353**	**Millipore**
mouse anti-α-SMA	**ab7817**	**Abcam**
mouse anti mouse IgG1	**5415**	**Cell Signaling Technology**
mouse anti mouse IgG2a	**61656**	**Cell Signaling Technology**
mouse anti human IgG2a	**ab200699**	**Abcam**
rabbit anti human IgG	**ab195574**	**Abcam**
Flow:		
Mouse TGF-β RI/ALK-5	**FAB5871A-100**	**R&D Systems**
APC-conjugated Antibody		
Rat IgG2A Allophycocyanin Isotype	**IC006A**	**R&D Systems**
Control		
Secondary antibody:		
WB:		
anti-mouse IgG HRP-linked Ab	**7076**	**Cell Signaling Technology**
anti-rabbit IgG HRP-linked Ab	**7074**	**Cell Signaling Technology**
IF:		

goat anti-mouse IgG Alexa 488	**A11001**	**Invitrogen**
goat anti-rabbit IgG Alexa 488	**A11008**	**Invitrogen**
goat anti-rabbit IgG Alexa 555	**A21428**	**Invitrogen**
goat anti-mouse IgG Alexa 555	**A21422**	**Invitrogen**
goat anti-rat IgG Alexa 488	**A11006**	**Invitrogen**
goat anti-rat IgG Alexa 555	**A21434**	**Invitrogen**